

SCREENING CRITERIA FOR SKIN CONTAMINATION IN A RADIOLOGICAL EMERGENCY

A Thesis
Presented to
The Academic Faculty

By

Caleigh E. Samuels

In Partial Fulfillment
of the Requirements for the Degree
Masters of Science in Medical Physics in the
School of Mechanical Engineering

Georgia Institute of Technology

August 2018

Copyright © Caleigh E. Samuels 2018

SCREENING CRITERIA FOR SKIN CONTAMINATION IN A RADIOLOGICAL EMERGENCY

Approved by:

Dr. Nolan E. Hertel, Advisor
School of Nuclear and Radiological
Engineering
Georgia Institute of Technology

Dr. Armin Ansari, Co-Advisor
Radiation Studies Branch
*Centers for Disease Control and
Prevention*

Dr. Chris Wang
School of Nuclear and Radiological
Engineering
Georgia Institute of Technology

Date Approved: April 23, 2018

ACKNOWLEDGEMENTS

First and foremost, I would like to express my deepest appreciation to Dr. Nolan Hertel for the opportunities he has afforded to me. I owe my success to his unwavering guidance and unrelenting support. Second, I would like to extend my profound gratitude to Dr. Armin Ansari whose contribution to this research endeavor cannot be overestimated. The completion of my thesis would not have been possible without his extensive knowledge and invaluable insight. I would like to extend my sincere thanks to Dr. Chris Wang for his advice. The lessons I have learned from him have been priceless. I also wish to thank Brooke Buddemeier who continues to provide me with encouragement and valuable advice. His insightful suggestions and extensive experience were invaluable to this research effort. I am additionally grateful to Lauren Finklea who was instrumental in keeping the project focused. I gratefully acknowledge the assistance of my colleagues at the Office of Radiological Safety at Georgia Tech who provided practical knowledge. Finally, I would like to recognize the help of my fellow students, specifically John Stooksbury, Jake Inman, and Greg Szalkowski, who often discussed my work with me and offered constructive criticism.

TABLE OF CONTENTS

Acknowledgments	iii
List of Tables	vii
List of Figures	ix
Chapter 1: Introduction	1
Chapter 2: Background	2
2.1 Health Risks Associated with Skin Contamination	2
2.2 Epidermal Thickness	3
2.3 Forms of Radiation	4
2.3.1 Gamma-rays	4
2.3.2 Alpha Particles	5
2.3.3 Beta Particles and Electrons	6
2.4 Geiger-Mueller Detectors	7
2.4.1 Detection Efficiency	7
2.5 Anticipated Exposure Time	9
2.6 Volume Effects of the Skin	9
2.7 Current Suggested Screening Levels	10

2.7.1	Federal Emergency Management Agency (FEMA)	11
2.7.2	Conference of Radiation Control Program Directors (CRCPD) . . .	13
2.7.3	Environmental Protection Agency (EPA)	13
2.7.4	International Atomic Energy Agency (IAEA)	14
2.7.5	National Council on Radiation Protection and Measurements (NCRP)	14
Chapter 3: Methods		17
3.1	Modified PiMAL Phantom	17
3.2	GM Pancake Probe Model	18
3.2.1	Model Verification	19
3.3	Contamination Model	19
3.4	Monte Carlo Simulations of Variation Due to Assumed Factors in Sug- gested Screening Criteria	20
3.4.1	Variation in Epidermal Thickness	20
3.4.2	Variation in Radionuclide Present	21
3.4.3	Variation in Source-to-Detector Distance	22
3.4.4	Variation in Extent of Contamination	22
3.4.5	Variation in Exposure Time	22
3.5	Relationship Between Dose and Detector Response	23
Chapter 4: Results		25
4.1	Pancake Probe Model Verification	25
4.2	Variation Associated with Epidermal Thickness	26
4.3	Variation Associated with Radionuclide Present	30

4.4	Variation Associated with Source-to-Detector Distance	35
4.5	Variation Associated with Extent of Contamination	39
4.6	Variation Associated with Exposure Time	46
4.7	Comparison of Variation in Assumed Factors	47
4.8	Comparison of Suggested Screening Criteria	49
Chapter 5: Conclusion and Future Work		52
Appendix A: Sample MCNP Input File		54
References		106

LIST OF TABLES

2.1	Suggested screening criteria	12
2.2	Response Factor of Baseline Beta Monitoring Instrument	15
4.1	Energy deposited per decay vs. epidermal thickness for Cs-137/Ba-137m skin contamination	27
4.2	Dose rate to the dermis vs. epidermal thickness for Cs-137/Ba-137m skin contamination	29
4.3	Detection efficiency vs. contamination radionuclides	31
4.4	Energy deposition per particle vs. contamination radionuclides	32
4.5	Dose rate to the dermis from skin contamination corresponding to a 1000 cpm detector response vs. contamination radionuclides	34
4.6	Detection efficiency of Cs-137/Ba-137m skin contamination vs. source-to-detector distance	35
4.7	Energy imparted per decay vs. source-to-detector distance for Cs-137/Ba-137m skin contamination	36
4.8	Dose rate vs. source-to-detector distance for Cs-137/Ba-137m skin contamination	38
4.9	Detection efficiency of Cs-137/Ba-137m skin contamination for a pancake GM probe with a 15 cm ² window vs. contamination area	40
4.10	Energy imparted per decay vs. contamination area for Cs-137/Ba-137m skin contamination	42
4.11	Dose rate vs. contamination area for Cs-137/Ba-137m skin contamination	44

4.12	Absorbed dose from Cs-137/Ba-137m skin contamination eliciting a 1000 cpm detector response vs. exposure time	46
4.13	Absorbed dose from Cs-137/Ba-137m spot contamination with the direct application of suggested generic screening criteria	50

LIST OF FIGURES

2.1	Skin structure	3
3.1	3D view and coronal section of the modified female Phantom with Moving Arms and Legs (PiMAL) Version 4.1 phantom.	18
3.2	Tc-99 and Cs-137 source used for model verification	20
3.3	Experimental setup for pancake probe model verification	20
3.4	Top: Cross-section pancake probe model verification simulation setup with Cs-137 source. Bottom: 3D rendition of HP260 pancake probe model verification simulation setup	20
4.1	Change in Cs-137/Ba-137m beta detection efficiency, gamma detection efficiency, and total detection efficiency with respect to epidermal thickness	26
4.2	Energy deposited in the dermis per decay from Cs-137/Ba-137m skin contamination as a function of epidermal thickness.	28
4.3	Average dose rate to the dermis from Cs-137/Ba-137m skin contamination eliciting a 1000 cpm detector response as a function of epidermal thickness	29
4.4	Change in detection efficiency with respect to radionuclides present	31
4.5	Change in energy deposition with respect to radionuclides present	33
4.6	Average dose rate to the dermis from skin contamination eliciting a 1000 cpm detector response with respect to radionuclides present	34
4.7	Change in Cs-137/Ba-137m beta detection efficiency, gamma detection efficiency, and total detection efficiency with respect to source-to-detector distance	36

4.8	Change in average energy deposited in the dermis from Cs-137/Ba-137m skin contamination with respect to source-to-detector distance	37
4.9	Average dose rate to the dermis from Cs-137/Ba-137m skin contamination eliciting a 1000 cpm detector response with respect to source-to-detector distance	38
4.10	Change in Cs-137/Ba-137m beta detection efficiency, gamma detection efficiency, and total detection efficiency with respect to extent of contamination. The area of the detector window (15 cm^2) is indicated with the vertical dotted line.	41
4.11	Change in energy imparted per decay from Cs-137/Ba-137m skin contamination with respect to extent of contamination. The vertical dashed line represents the area of the defined dose volume (10 cm^2).	43
4.12	Average dose rate to the dermis from Cs-137/Ba-137m skin contamination eliciting a 1000 cpm detector response with respect to extent of contamination. The vertical dashed line represents the area of the defined dose volume (10 cm^2). The area of the detector window (15 cm^2) is indicated with the vertical dotted line.	45
4.13	Change in absorbed dose to the dermis from skin contamination eliciting a 1000 cpm response at 1 cm with respect to exposure time	47
4.14	Top left: Change in average dose rate to the dermis from Cs-137/Ba-137m skin contamination eliciting a 1000 cpm detector response with respect to epidermal thickness. Bottom left: Change in average dose rate to the dermis from Cs-137/Ba-137m skin contamination eliciting a 1000 cpm detector response with respect to source-to-detector distance. Top right: Change in average dose rate to the dermis from skin contamination eliciting a 1000 cpm detector response with respect to contamination source. Bottom right: Change in average dose rate to the dermis from Cs-137/Ba-137m skin contamination eliciting a 1000 cpm detector response with respect to contamination extent.	48

SUMMARY

In response to a nuclear or radiological emergency, potentially contaminated individuals are screened for external contamination[1, 2]. During the screening process, a threshold screening level is used to triage into two groups: one consisting of those individuals who need to be decontaminated and the other consisting of those who are either uncontaminated or will be given instructions for self-decontamination. Several organizations have suggested generic contamination levels for this threshold. However, differing assumptions made during the development of these values regarding the radionuclides present, the distance between the contaminated surface and the detector, the extent of contamination, the detector type, etc. have led to potential inconsistencies among the suggested screening values.

This study uses a modified Phantom with Moving Arms and Legs (PiMAL) phantom and an experimentally verified Geiger-Mueller (GM) pancake probe modeled in the MCNP6 (Monte Carlo N-Particle 6) transport code to examine the effects of these differing assumptions on the dose received by a contaminated individual. A 5 μm layer of contamination was modeled to be in direct contact with the epidermis of the phantom. Five sets of models were created. Each set independently varies either the thickness of the epidermis, radionuclides comprising the contamination, distance between the probe and the contamination, extent of contamination, or exposure time. The amount of activity assumed to be present was such that it elicited a detector response of 1000 counts per minute (cpm) for each model. In each scenario, the relationship between the absorbed dose in a 10 cm^2 area of the dermis centered below the contamination and the pulse rate produced in the pancake probe was analyzed.

CHAPTER 1

INTRODUCTION

Nuclear and radiological incidents are generally regarded as low-probability, high-consequence events. Between 1944 and 2000, there were 243 serious accidents in the United States reported to the Radiation Emergency Assistance Center/Training Site (REAC/TS) Registry[3]. Instabilities of nuclear states, vulnerabilities of nuclear power plants, availability of radioactive materials leading to possible terrorism, and growth in industrial use of radioactivity present the possibility of a nuclear or radiological emergency[4, 5, 6].

In the event of a nuclear or radiological emergency, potentially contaminated individuals are screened for external contamination[1, 2]. During this process, screening criteria are used to delineate those who require decontamination from those who will either be given instructions for self-decontamination or are not contaminated. Several organizations have suggested generic screening criteria to be used in such a scenario. However, assumptions made regarding characteristics of the contamination, the radiation detection instrument, and the individual being screened has led to inconsistencies among the suggested criteria.

This research focuses on analyzing the effects of variation in assumptions made during the development of external screening criteria on the dose received by a contaminated individual during a nuclear or radiological incident. Five factors were evaluated: epidermal thickness, contamination source, separation between the contaminated skin and the detector probe, extent of the contamination, and exposure time. Monte Carlo simulations were used to determine the effect of each factor on the relationship between the detector response and the absorbed dose to the dermis of a contaminated individual.

CHAPTER 2

BACKGROUND

Several organizations have suggested generic screening criteria for external contamination during radiological and nuclear emergencies. In deriving these suggested criteria, several assumptions were made regarding characteristics of the detector, the human body, and the contamination itself. In order to understand the dose a contaminated individual may receive given a screening value, one must understand the effects of these characteristics on the relationship between the dose received and the detector response.

2.1 Health Risks Associated with Skin Contamination

The purpose of screening potentially contaminated individuals is to protect the public from potential mental and physical health effects that could result from skin contamination[7, 8]. The primary goal of screening is to avoid deterministic effects, those effects in which the severity of the effect is dependent on the dose[1]. All deterministic effects are associated with a dose threshold below which the effect will not occur. Radiation Emergency Assistance Center/Training Site (REAC/TS) lists dose thresholds of 3 Gy for epilation, 6 Gy for erythema, 10-15 Gy for dry desquamation, 15-25 Gy for moist desquamation, and greater than 25 Gy for ulceration [9]. IAEA SRS-02 provides similar dose threshold estimates of less than 3 Gy for epilation, 3 to 10 Gy for erythema, 8 to 12 Gy for dry desquamation, 15 to 20 Gy for moist dequamation, 15 to 25 Gy for blister formation, and greater than 20 Gy for ulceration [10].

The secondary goal is to minimize the probability of stochastic effects (e.g. radio-carcinogenesis). Of the possible stochastic effects, radiation-induced skin cancer is the primary concern with external contamination. Studies have shown the excess relative risk of skin cancer incidence to be approximately 10 percent per Sv (0.1 percent per rem) for

acute doses [9, 11].

2.2 Epidermal Thickness

The human skin is made up of several layers including an outer protective layer of dead or dying cells referred to as the epidermis[12]. Energy deposited in these dead cells does not cause any harmful effects to the person. The outermost, exposed layer of the epidermis is referred to as the stratum corneum. This layer is made up entirely of dead cells which are pushed to the top and sloughed off. The basal layer, a single layer of cells capable of cell division, lays directly below the epidermis separating the epidermis from the dermis[12]. This is the outermost layer of viable cells. Unlike the epidermal cells, radiation damage to these cells can lead to harmful health effects. Below the basal layer lies the dermis, often referred to as the "true skin"[12]. Similarly to the basal layer, the dermis contains viable tissue which is sensitive to radiation. Figure 2.1 depicts the layers of the discussed layers of the skin.

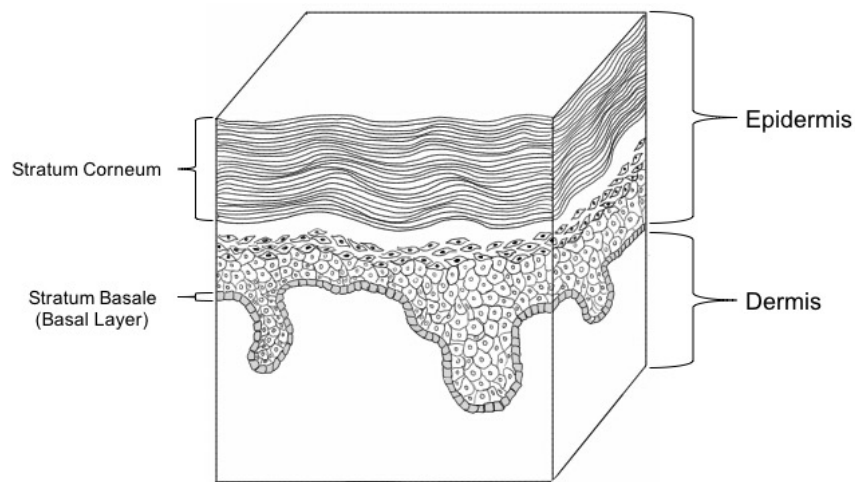


Figure 2.1: Skin structure

Current dosimetry calculations assume the epidermal thickness to be $70\text{ }\mu\text{m}$ (7 mg/cm^2) [13, 14]. However, this is an oversimplified assumption. Epidermal thickness varies not only from person to person, but also from one body site to the next [14, 15, 16]. Average

epidermal thickness of the trunk has been measured to be $47\text{ }\mu\text{m}$ (4.7 mg/cm^2) whereas average epidermal thickness on the fingertips has been measured to be $406\text{ }\mu\text{m}$ (40.6 mg/cm^2). The thinnest recorded epidermal thickness was found on the temple and measured $17\text{ }\mu\text{m}$ (1.7 mg/cm^2) thick. The thickest recorded epidermal thickness was found on the fingertip and measured $485\text{ }\mu\text{m}$ (48.5 mg/cm^2) thick [14]. However, several sources state that the sole of the foot is approximately 1400 or $1500\text{ }\mu\text{m}$ [17, 18, 19].

In addition to variations with body site, epidermal thickness on the arms and legs has been found to increase with age and the epidermal thickness on the face tends to be thinner in females than in males [14]. Evidence has also been found indicating a variation of epidermal thickness due to environmental factors. The more exposed to the environment the skin is, the thicker the epidermis becomes[14]. Extended smoking habits correlate to thinner epidermal thicknesses[16]. Additionally, increased pigmentation has been correlated to increased epidermal thickness[16]. Due to these variations in epidermal thickness, it has been suggested that $40\text{ }\mu\text{m}$ be considered the average epidermal thickness for dosimetry calculations rather than the currently assumed $70\text{ }\mu\text{m}$ [15]. For various applications, the ICRP has applied epidermal thickness from $20\text{ }\mu\text{m}$ to $100\text{ }\mu\text{m}$ in dosimetry calculations [20]. However, the ICRP recommends the use of $70\text{ }\mu\text{m}$ for general dosimetry calculations, as the majority of the epidermis is between 50 and $100\text{ }\mu\text{m}$ thick [21].

2.3 Forms of Radiation

Various types of nuclear and radiological incidents will introduce different isotopes with various forms of radiation into the environment. The ability of a particle to penetrate either the detector or the epidermal layer of the skin is dependent on the particle type and energy.

2.3.1 Gamma-rays

Gamma-rays lose energy through three interactions, photoelectric effect, Compton scattering, and pair production. In these interactions, the gamma-ray transfers energy to the

medium by producing secondary electrons. The secondary electrons produced in gamma-ray interactions are responsible for the deposited energy in the material.

The photons themselves can travel relatively large distances in matter before interacting. The mean free path of a photon for a given material is defined as the average distance a photon will travel before interacting in the material. Practically, the energy of a gamma ray can range from approximately 2.6 keV to 7.1 MeV [22]. In air, this equates to a mean free path from 0.027 m to 352 m, respectively. In soft tissue, this equates to a mean free path from approximately 37 μm to 38 cm, respectively. A gamma-ray must have a kinetic energy of approximately 3.4 keV in order to have a mean free path of 70 μm in soft tissue. This means that on average, a gamma-ray with 3.4 keV will penetrate a 70 μm epidermis before interacting. In order to have a mean free path of 17 μm in soft tissue, a gamma-ray only requires a kinetic energy of approximately 2 keV. Therefore, gamma-rays in the practical energy range will, on average, penetrate the thinnest epidermal thicknesses prior to interacting.

2.3.2 Alpha Particles

Alpha particles have a high amount of energy imparted to the medium per unit track length of the particle, or rather, a high linear energy transfer (LET). Naturally occurring radionuclides emit alpha particles with kinetic energies between 4 and 8 MeV[23]. However, the most common alpha emitters only have kinetic energy between 4.5 and 5.5 MeV[24]. Applying the Lapp and Andrews alpha particle range equation and the Bragg-Kleman rule, the range of a common alpha particle in tissue is approximately 30 μm to 41 μm . An alpha particle requires a minimum of 7.5 MeV to penetrate the average epidermal layer (70 μm)[24]. Therefore, practically, alpha particles will deposit all of their energy within the epidermis, the dead layer of skin, before reaching viable cells assuming a 70 μm epidermal thickness. However, for a 17 μm epidermal thickness, an alpha particle only requires a minimum of approximately 3.2 MeV in order to penetrate through the epidermal layer into the basal

layer, the outermost layer of viable cells. Practically, alpha particles are not hazardous to the human body unless they are internalized (inhaled, ingested, etc.). Internalized, alpha particles deposit large local doses leading to serious health consequences[25]. External contamination increases the probability of internalization of the contaminant[1].

2.3.3 Beta Particles and Electrons

For beta particles and electrons, LET is inversely proportional to the particle's energy. Overall, beta particles and electrons have a relatively low LET. The probability of a beta particle or electron penetrating the skin is highly dependent on the energy of the particle. Unlike alpha particles, beta particles emitted from radioactive decay are not monoenergetic, but rather are emitted within an energy spectrum. The range of a beta particle in a given media is the expectation value of its total pathlength in the media before depositing the entirety of its kinetic energy and coming to a rest. The continuous-slowing-down approximation (CSDA) range is an approximation of the particle's range assuming that the particle loses energy at a constant rate. The projected range of the particle in a given medium is the expectation value of the maximum depth of penetration within the medium.

For low energy electrons, the CSDA range is approximately equivalent to the projected range of the particle[22]. CSDA range tables indicate that a beta particle requires a kinetic energy of approximately 70 keV in order to penetrate the average epidermal layer of the skin (70 μm)[22, 26]. As a rule of thumb, the average energy of a beta spectrum is approximately equal to one third of the maximum beta energy. However, not all beta spectra follow the same energy distribution. For example, although the maximum energy of I-131 and Cs-137 beta particles are 807 keV and 1170 keV, respectively, the mean beta energies of I-131 and Cs-137 are 181 keV and 188 keV, respectively. While a high-energy beta particle is both an internal and an external hazard, a low energy beta particle will deposit all of its energy in the epidermis. All beta emitters will produce some beta particles that fall into this low energy category. Some beta emitters, such as H-3, have a maximum beta energy below

the minimum energy required to penetrate the epidermis. Similarly to alpha emitters, these low energy beta emitters are not a hazard unless internalized.

2.4 Geiger-Mueller Detectors

Geiger-Mueller (GM) detectors are commonly available in emergencies due to their simplicity, ease of use, affordability, and widespread use in performing contamination surveys[27, 28].

2.4.1 Detection Efficiency

When setting criteria for portable instruments, one needs to understand the several factors affecting detection efficiency. Changes in either the intrinsic efficiency and the geometric efficiency will impact the detector response to radiation.

Intrinsic Efficiency

Intrinsic efficiency is the ratio between the number of pulses recorded and the number of radiation quanta incident on the detector. The intrinsic efficiency is highly dependent on the properties of the incident radiation. Only one ion pair must be formed in the fill gas to spark a Geiger discharge. Therefore, the intrinsic efficiency for charged particles is close to 100 percent. However, due to the low interaction probability of gamma-rays, it is extremely uncommon for a gamma-ray to interact in the detector fill gas. In order to start a Geiger discharge, the gamma-ray typically must interact in the detector wall to create a secondary electron and the secondary electron must reach the fill gas. For this reason, the intrinsic efficiency for a GM is only a few percent at most for gamma-rays[28].

Geometric Efficiency

Geometric efficiency accounts for all geometric factors. This can include the solid angle subtended by the detector with respect to the source, interaction with material between the

source and the detector, backscatter, etc.[29]. When screening for external contamination, the geometric factor leading to the greatest loss in detection efficiency is the solid angle. Suggested screening criteria instruct emergency response personnel to hold the probe at various distances from the potentially contaminated skin surface while screening individuals. This distance can range between 1 cm and 2.54 cm. Response personnel assigned to screen potentially contaminated individuals typically include volunteers with minimal training. This often leads to an increase in the distance between the potentially contaminated skin surface and the detector probe of several centimeters or more. Typically, manufacturers report the 2π efficiency, the count rate of the detector divided by the activity emitted in a solid angle of 2π (half of the total activity for an isotropic source)[30].

For this situation, typically the only materials between the contamination and the detector is air and parts of the detector itself, mainly the detector window. As beta particles are low LET, they can typically pass through the detector window before depositing all of their energy. However, as previously mentioned, beta decay produces beta particles with a distribution of energies. Those with low energy will be preferentially absorbed in the detector window, never reaching the fill gas and producing a pulse. Therefore, practical beta efficiencies are much lower than 100 percent. A few isotopes, such as H-3 and C-14, produce beta particles with such a low energy spectrum that the large majority of the particles are absorbed in the detector window causing the detection efficiency to be practically zero. The detector window of a pancake GM is made of polyethylene terephthalate, also known as mylar. This material has a low effective mass number, therefore, bremsstrahlung creation in the detector window is insignificant for beta particles and electrons below 10 MeV. As alpha particles are high LET, there can be significant absorption and backscatter from the detector window causing a significant drop in the total detection efficiency as the window thickness increases.

2.5 Anticipated Exposure Time

The anticipated exposure time, or time that the contamination will remain on the skin, must also be taken into account. For fixed contamination (contamination that is not cleaned by repeated washing), the exposure time is assumed to be 14 days after the contamination incident. This is the estimated time that it will take for a cell at the base of the stratum corneum, the outermost, dead layer of the epidermis, to reach the surface and be sloughed off [31, 32]. For loose (removable) contamination, the exposure time is anticipated to be the time between the contamination event and decontamination by the removal of contaminated clothes and washing[1]. In the event of a radiological or nuclear emergency, the public may be instructed to stay inside for the first 12 to 24 hours while radiation levels decrease and emergency responders mobilize[33]. This will cause a delay between the contamination event and the screening and decontamination of potentially contaminated individuals. Factors such as availability of water, the size of the population involved, or the availability of instruments can alter the ability to effectively screen and decontaminate individuals and therefore alter the exposure time for an individual[1]. For example, during the screening of those affected by the Fukushima accident, responders were faced with difficulties in obtaining water for decontamination[8]. Therefore, the exposure time for loose contamination is typically assumed to be between one and two days. The generic screening criteria suggested by various agencies assumes exposure times of 12 hours, 24 hours, or 36 hours for loose contamination.

2.6 Volume Effects of the Skin

The extent of contamination has two major effects in determining a screening criteria. First, it can have a great effect on the solid angle and, therefore, a large impact on the detector efficiency. Secondly, for small irradiation volumes (i.e. skin contamination areas), the skin displays a volume effect[34, 35, 36]. That is to say, that in comparison to uniform

contamination over a large skin surface, the skin is able to tolerate larger doses in smaller volumes before demonstrating a specific health effect. This volume effect is thought to be caused by the skin's methods of repairing the damaged area. The current hypothesis is that there are three repair mechanisms of the skin: migration and division of viable cells from the basal layer, migration and division of viable cells from hair follicles, and migration and division of viable cells from the perimeter of the damaged area[34]. The repair of large area skin injuries is driven by the first two repair mechanisms. The third mechanism is unable to significantly contribute to repair of large area damage due to the slow pace of cell migration (approximately 0.2 mm/day)[35, 37]. However, if the damaged area is small enough, the third mechanism plays a significant role in enabling the skin to repair the damage more quickly. Therefore, more cells must be damaged in order for a given deterministic effect to occur.

2.7 Current Suggested Screening Levels

Several organizations have published suggested screening criteria for skin contamination including Conference of Radiation Control Program Directors (CRCPD), Environmental Protection Agency (EPA), Federal Emergency Management Agency (FEMA), International Atomic Energy Agency (IAEA), and National Council of Radiation Protection and Measurement (NCRP). These criteria are summarized in Table 2.1. Some of the suggested screening criteria are based on minimizing stochastic effects while others are based on preventing deterministic effects. Inconsistent units are used across organizations, including counts per minute (cpm), counts per second (cps), Bq/cm², dpm/cm², and Sv/h. They also use inconsistent terminology. Some have “decontamination level” and “release levels”, while others have “screening values”, “operational intervention levels”, or “required decontamination levels” and “recommended decontamination levels”. In the derivation of the criteria, the organizations used differing assumptions as to the detector type, the involved radionuclides, the source-to-detector distance, the extent of the contamination, and

the exposure time.

2.7.1 Federal Emergency Management Agency (FEMA)

FEMA suggests screening criteria for contamination of the skin during nuclear power plant accidents. In FEMA-REP-21 it is suggested that an individual with widespread contamination under 1 μCi will not be at significant risk of any detrimental health effects[38]. Furthermore, it is suggested that no more than 10% of this contamination (0.1 μCi) will be concentrated in a small area (0.2 cm^2). FEMA-REP-22 utilizes these values to suggest screening criteria based on the detector response of portable instruments[39]. FEMA-REP-22 sets a 'recommended decision criteria' of 300 cpm above background for fixed contamination, contamination that is not readily removable, on the skin. If loose and fixed contamination is present, FEMA-REP-22 recommends a decision criteria of 3,000 cpm above background. These decision criteria assume the use of a CD V-700¹ meter with a standard side window GM (the least sensitive instrument tested by FEMA). The FEMA-REP-22 background documentation recommends increasing the decision criteria to 10,000 cpm above background for fixed contamination (100,000 cpm above background for loose and fixed contamination) when using a modern instrument with a pancake GM probe[40]. It is assumed that the exposure time for loose contamination is 36 hours (12 hours before monitoring and 24 hours after monitoring) and 14 days for fixed contamination as this is the approximate time required for the skin to naturally replace itself. The detector housing is assumed to be one inch away from the skin. FEMA bases the decision criteria on a Cs-137/Ba-137m source as the average beta energy from this source is similar to the average beta energy from the predicted mix of radionuclides released in a major nuclear power accident.

¹Manufactured by Nuclear Research Corporation between 1954 and 1955, Victoreen Instrument Company between 1956 and 1962, International Pump and Machine Works Inc. in 1957, Chatham Electronics in 1957, Anton Electric Laboratories, Inc. between 1959 and 1960, Lionel Electronic Laboratories between 1960 and 1962, and Electro-Neutronics Inc. in 1962

Table 2.1: Suggested screening criteria

Documentation	β/γ Screening Criteria	Contamination Radionuclide	Skin-to-Detector Separation	Contamination Extent	Exposure Time
FEMA-REP-22 [1]	1,000 cpm fixed/ 10,000 cpm loose above background	Cs-137/Ba-137m	2.54 cm	0.2 cm ² spot with widespread	14 days fixed/ 36 hours loose
CRCPD Handbook [1]	10,000 cpm above background	Cs-137/Ba-137m	2.54 cm	Widespread	Not specified
EPA 2017 PAG Manual [1]	2 × background	Not specified	Not specified	Not specified	12 hours
IAEA EPP-NPR-OILs 2017 [1]	β : 1,000 cps γ : 1 μ Sv/h	LWR emergency mix	β : 2 cm γ : 10 cm	Not specified	Not specified
NCRP Report No. 161 [1]	10,000 Bq/cm ² (1,000 Bq/cm ²)	Sr-90	1 cm	0.2 cm ² spot with widespread	Not specified
NCRP Report No. 165 [1]	600,000 dpm/cm ²	Sr-90	1 cm	Not specified	Not specified (>6-12 hours)
NCRP Report No. 166 [1]	1,000 cpm	Sr-90	1 cm	Not specified	24 hours

2.7.2 Conference of Radiation Control Program Directors (CRCPD)

CRCPD documentation was designed to be used in the event of a radiological dispersal device (RDD) for the purpose of minimizing the risk of stochastic effects[41]. CRCPD recommends a release level of 1,000 cpm below which people can be instructed to go home and shower. In situations involving resource limitations or large populations, CRCPD suggested that the release level may be raised to 10,000 cpm above background. These levels are meant to be used when measuring 1 inch away from the contamination using a pancake GM probe. In the derivation of CRCPDs screening criteria, Cs-137/Ba-137m was assumed to be the radionuclide involved. No exposure time was specified.

2.7.3 Environmental Protection Agency (EPA)

EPA has published several documents in which they present suggested screening criteria, including Protective Action Guides (PAGs) [42]. Their most recent guidance, 2017 PAG Manual, recommends a decontamination level of greater than two times the existing background level and a release level of less than two times the existing background[42]. These levels are intended to be applicable to any emergency involving a significant release of radionuclides. They are “derived primarily on the basis of easily measurable radiation levels using portable instruments.” Although prior guidance from the EPA has assumed the use of a thin window GM, the latest PAG Manual does not specify the use of any given detector[43]. Previous guidance has also stated that the screening criteria were derived using an assumed exposure time of 12 hours before decontamination; however, the latest guidance from the EPA does not disclose an assumed exposure time. The radionuclides involved, source to detector distance, and extent of contamination assumed in the development of this PAG are not specified.

2.7.4 International Atomic Energy Agency (IAEA)

IAEA presents default values, called Operational Intervention Levels (OILs), above which specified protective actions are to be taken[44]. $OIL4_{\beta}$ and $OIL4_{\gamma}$ provide screening criteria for skin monitoring of beta and gamma radiation, respectively. $OIL4_{\beta}$ sets a default screening criteria of 1,000 cps at 2 cm away from the hands and face for beta particles. The default $OIL4_{\beta}$ criterion was derived using a baseline beta monitoring instrument, a beta monitoring instrument with an effective window area of 15 cm² and an efficiency corresponding to the ideal response factors provided in EPR-NPP-OILs 2017, displayed in Table 2.2. Although this default value is conservatively applicable to any beta monitoring instruments typically used for beta monitoring on the skin, guidelines are provided to calculate instrument specific $OIL4_{\beta}$ levels. $OIL4_{\gamma}$ sets a default screening criteria of 1 Sv/h at 10 cm away from the hands and face for gamma-rays. Use of $OIL4_{\gamma}$ is preferred over $OIL4_{\beta}$ as it is ‘less dependent on monitoring technique and instrument characteristics.’ In the derivation of both $OIL4_{\beta}$ and $OIL4_{\gamma}$, all radionuclides that are of concern during an LWR emergency were considered. IAEA applies a weighting factor of 0.5 to the derivation of both $OIL4_{\beta}$ and $OIL4_{\gamma}$ in order to account for inhalation, ingestion, and operational practicality. The extent of the contamination and the exposure time assumed in the derivation are not specified. IAEA also suggests that higher $OIL4_{\beta}$ and $OIL4_{\gamma}$ may be used in situations involving large populations or resource limitations.

2.7.5 National Council on Radiation Protection and Measurements (NCRP)

The NCRP has multiple documents regarding screening criteria.

NCRP Report No. 161

NCRP Report No. 161 is intended to be applicable to a wide variety of incidents in which people may be contaminated[45]. The screening criteria suggested in this report are intended to be used only in the absence of a screening value provided by the ‘national com-

Table 2.2: Response Factor of Baseline Beta Monitoring Instrument

(Adapted from EPR-NPP-OILs 2017)

Radionuclide	Response Factor (cps/Bq))	Radionuclide	Response Factor (cps/Bq))
P-32	1.5E-01	I-133	1.4E-01
Cl-36	1.3E-01	I-134	1.5E-01
Rb-86	1.4E-01	I-135	1.3E-01
Sr-89	1.4E-01	Cs-134	8.8E-02
Sr-90	2.6E-01	Cs-136	1.1E-01
Sr-91	1.4E-01	Cs-137	1.3E-01
Y-91	1.4E-01	Ba-140	3.0E-01
Zr-95	1.5E-01	Ce-141	1.4E-01
Zr-97	2.9E-01	Ce-143	1.4E-01
Mo-99	1.5E-01	Ce-144	2.3E-01
Ru-103	5.2E-02	Pr-143	1.3E-01
Ru-105	1.7E-01	Nd-147	1.3E-01
Ru-106	1.5E-01	Np-239	2.0E-01
Rh-105	1.0E-01	Pu-238	1.5E-04
Te-127m	2.1E-01	Pu-239	5.8E-05
Te-127	1.2E-01	Pu-240	1.2E-04
Te-129m	1.9E-01	Pu-241	1.2E-06
Te-131m	1.2E-01	Am-241	5.0E-04
Te-132	2.1E-01	Cm-242	6.1E-05
I-131	1.2E-01	Cm-244	4.6E-05

petent authority.’ Under these circumstances, NCRP Report No. 161 suggests adopting the 2005 IAEA OILs. In accordance with these OILs, it is suggested that individuals with contamination below 100 Bq/cm² be released. Those with contamination between 100 Bq/cm² and 1,000 Bq/cm² should be released with instructions to shower and wash their clothes. This report recommends that the decontamination level be set at 1,000 Bq/cm², above which individuals should be decontaminated on site. NCRP Report No. 161 suggests that this decontamination level may be increased; however, it is recommended that the decontamination level does not exceed 10,000 Bq/cm². In accordance with prior NCRP documentation and FEMA-REP-22, this report suggests giving decontamination priority to any individual with contamination greater than 37,000 Bq on a 0.2 cm² spot of skin. NCRP Report No. 161 suggests these values under the assumption that while screening

an individual, the detector probe is held at a distance of 1 cm from the skin and the probe is scanned across the skin at a speed of 3 to 5 cm/s. Although not explicitly stated in this documentation, this screening criteria is based on Sr-90 contamination.

NCRP Report No. 165

NCRP Report No. 165 is intended for use during nuclear and radiological terrorism incidents (RDD, RED, IND, etc.)[46]. In this report, NCRP emphasizes the need to adapt the screening level in response to the size of the incident. However, the report suggests an upper limit for the screening level of 600,000 dpm/cm² for beta/gamma contamination. Although the assumed exposure time is not stated, in this report the NCRP states that it should take 6 to 12 hours to establish an appropriate screening center. Although not explicitly stated in this documentation, this screening criteria is based on Sr-90 contamination and the separation between the detector probe and contaminated surface was assumed to be 1 cm.

NCRP Report No. 166

NCRP Report No. 166 is intended to be applied to nuclear or radiological events in which a population may be exposed, specifically large-scale events[47]. This report suggests a screening criteria of 1,000 cpm using a pancake probe GM. However, as in NCRP Report No. 165, this document stresses the need to scale the screening value in response to the size of affected population. NCRP Report No.166 suggests this criteria under the assumption that the surveyor is holding the probe approximately 1 cm away from the skin and scanning at approximately 3 to 5 cm/s. In deriving the suggested screening criteria, Sr-90 was used as the model contamination source and there was an assumed exposure time of 24 hours, as it is anticipated that a Federal Radiological Monitoring and Assessment Center (FRMAC) will take 24 to 36 hours to become fully operational after the incident.

CHAPTER 3

METHODS

For this study, four sets of MCNP models were developed. In each set, either the thickness of the epidermis, the radionuclide present, the separation between the detector probe and the contaminated surface, or the extent of contamination was independently varied. All variability models consist of contamination modeled to be in direct contact with the skin of the phantom and a pancake GM probe positioned so that the detector window faces the contamination.

3.1 Modified PiMAL Phantom

The female PiMAL Version 4.1 phantom, developed by the United States Nuclear Regulatory Commission at Oak Ridge National Laboratory, was utilized in all models of this study. This phantom has been verified against tabulated dose conversion coefficients in ICRP Publication 74/ICRU Report 57 as well as computed organ dose values from the ORNL-UF and MIRD-5 phantoms[48]. The PiMAL phantom was chosen over the ORNL-UF and MIRD-5 phantoms due to the ease of the user to manipulate the position of the arms and legs. In each scenario, the phantom was modified to have two layers of skin: a dermis and an epidermis. The material assigned to both layers is consistent with the original phantom; therefore, this modification does not affect the interaction of particles with the phantom.

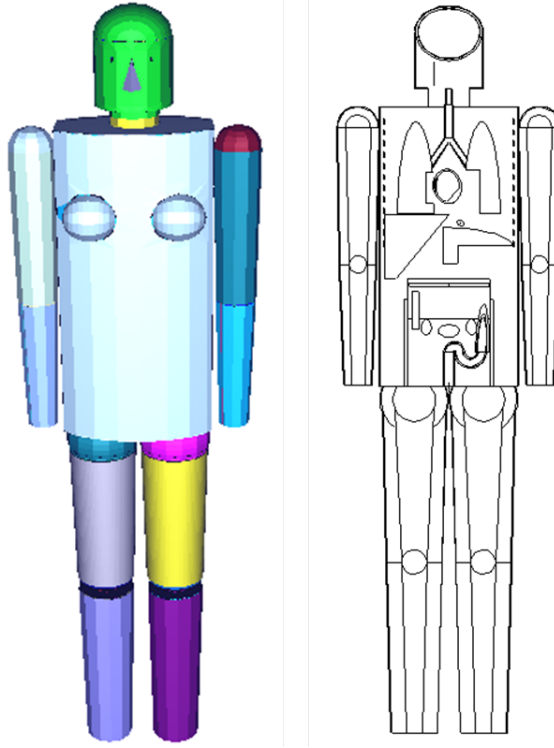


Figure 3.1: 3D view and coronal section of the modified female Phantom with Moving Arms and Legs (PiMAL) Version 4.1 phantom.

3.2 GM Pancake Probe Model

For the purposes of this study, a GM pancake probe was modeled as the detector. Although a wide range of detectors could be considered appropriate for contamination screening purposes, pancake GM probes are commonly available. The GM pancake probe model utilized in this work was modified from a model developed in prior work [49]. The geometry and materials of the original model were modeled using Ludlum and LND specifications of the HP-260 Pancake Probe and the Model 44-9 Pancake Probe. The fill gas was modified from the original model to be composed of Ne, Ar, and Br₂ in atomic fractions of 92%, 7.5%, and 0.5%, respectively. The fill gas pressure was modeled at 0.975 atm as to be in line with that experimentally determined by Bloch et al. [50].

3.2.1 Model Verification

Measurements using seven Ludlum Model 44-9 pancake probes with Ludlum Model 3 ratemeters were used to evaluate the accuracy of the MCNP model and simulation of a GM pancake probe. Two sources were used to verify the model: a NIST traceable sealed Cs-137 check source and an electroplated Tc-99 source. The Cs-137 source is mounted on a stainless steel disk, encapsulated in a plastic disk. The stainless steel disk is 0.10 mm thick and 1.27 cm in diameter. The plastic disk encapsulating the stainless steel disk is 1/8" thick and 1" in diameter. Both sources sit on stainless steel plates inside a plastic source holders, as shown in Figure 3.2. The exact materials of the holder are unknown. Therefore, in the Monte Carlo simulation, stainless steel 446 was used as the material composition for the metal and polyethylene was used as the material composition for the plastic. Four measurements were taken with each of the seven probes for each source. For these measurements, the probe was flush with the open end of the source holder, sitting approximately 3 mm above the source, as shown in Figure 3.3. The same setup was modeled in the MCNP simulation as can be seen in Figure 3.4. The efficiency was calculated from the average count rate for each source and compared to the calculated efficiency from the corresponding MCNP simulation.

3.3 Contamination Model

Air was chosen as the material for the contamination layer for two reasons. First, at the activity levels of interest for screening criteria, the atomic fraction of radioactive material is insignificant as compared to the atomic fraction of air in the contamination layer assuming a uniform distribution. Second, modeling the contamination as air provides a more conservative estimate of the dose deposited per detector response unit.

Several thicknesses of contamination were simulated in order to evaluate the impact of self attenuation on the relationship between the dose and detector response. The results in-

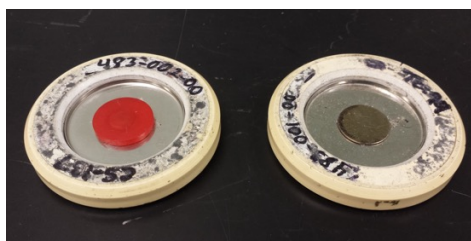


Figure 3.2: Tc-99 and Cs-137 source used for model verification



Figure 3.3: Experimental setup for pancake probe model verification

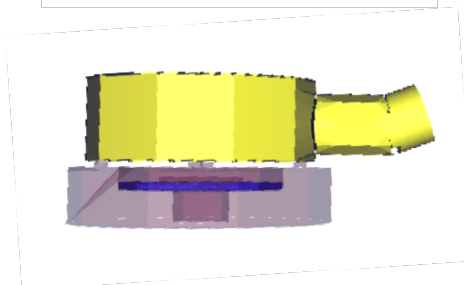
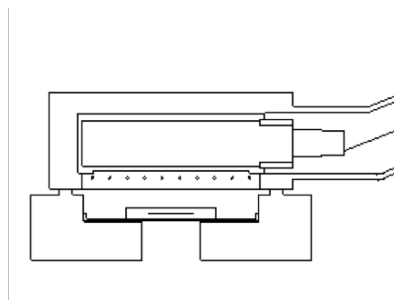


Figure 3.4: Top: Cross-section pancake probe model verification simulation setup with Cs-137 source. Bottom: 3D rendition of HP260 pancake probe model verification simulation setup

indicated that, at the activity levels in question, the effects of self absorption are insignificant. Therefore, it was deemed appropriate to model the thickness of the contamination layer as $5 \mu\text{m}$.

3.4 Monte Carlo Simulations of Variation Due to Assumed Factors in Suggested Screening Criteria

3.4.1 Variation in Epidermal Thickness

In order to study the impact of variation in the thickness of the epidermis, a set of five simulations was created. In each simulation, the thickness of the phantom's epidermis was modified. The thinnest epidermal thickness modeled was $17 \mu\text{m}$, as this is the thinnest experimentally reported epidermal thickness (found on the temple). The second simulation was modified to have a $40 \mu\text{m}$ thick epidermis; it was recommended by Whitton that this value should be used as the assumed average epidermal thickness for skin dose control cal-

culations. In the third simulation, the PiMAL phantom was modified to have a 70 μm thick epidermis; this is the currently assumed average epidermal thickness in skin dose calculations. In the fourth simulation, the PiMAL phantom was modified to have an epidermal thickness of 400 μm as to simulate the average thickness of the fingertips. In the final simulation of this set, the phantom was modified to have an epidermal thickness of 1500 μm in order to simulate the average epidermal thickness on the sole of the foot, the location of the thickest epidermal layer. In each of the models in this set, all other variables (the radionuclide present, separation between the detector probe and the contaminated surface, extent of the contamination, and the exposure time) were held at a constant assumed value. Cs-137/Ba-137m was assumed to be the only radionuclide involved, the exposure time was assumed to be 36 hours, and it was assumed that the only contamination present was a 0.2 cm^2 spot. The location of the detector probe was modified in each model in order to maintain an assumed separation between the probe and contaminated surface of 1 cm.

3.4.2 Variation in Radionuclide Present

The effects of the beta energy on the relationship between the detector response and the dose deposited was evaluated with a set of four MCNP simulations. Each one modeled the contamination as a singular beta emitter: either Tc-99, I-131, Cs-137/Ba-137m, or Sr/Y-90. Fission products, I-131, Cs-137, and Sr-90 are three of the main emissions to the environment from the 1986 Chernobyl Nuclear Power Plant accident[9]. Cs-137 and I-131 were also released during the 2011 Fukushima Daichi Nuclear Power Plant accident and Cs-137 was the sole contaminant in the 1987 Goiania incident[51]. The beta spectra of each source was modeled using the ICRP Publication 72 values taken from Radiological Toolbox Version 3.0.0 developed by Oak Ridge National Laboratory. The maximum beta energy emitted by Tc-99, Sr-90, I-131, Cs-137, and Y-90 are 294 keV, 546 keV, 807 keV, 1.17 MeV, and 2.28 MeV, respectively. All other variables were held constant across each model. The epidermal thickness was assumed to be 70 μm , the probe was modeled with a

separation of 1 cm from the contaminated surface, the exposure time was assumed to be 36 hours, and it was assumed that the only contamination present was a 0.2 cm² spot.

3.4.3 Variation in Source-to-Detector Distance

Five values of separation between the contaminated surface and the detector probe were evaluated in this work. The first three values, 1 cm, 2 cm, and 2.54 cm, are each considered proper screening procedure by at least one of the organization suggesting screening values. The fourth and fifth values, 5.08 cm (2") and 7.62 cm (3"), are considered bad practice; however, it is known that separation of this magnitude often occurs during the screening process. In each of the models of this set, all other variables were held at an constant assumed value. The epidermal thickness was held at 70 μ m, Cs/Ba-137 was assumed to be the only radionuclide involved, the exposure time was assumed to be 36 hours, and it was assumed that the only contamination present was a 0.2 cm² spot.

3.4.4 Variation in Extent of Contamination

Several simulations were used to evaluate the effects of contamination area on the relationship between detector response and dose to the dermis. For each simulation, the diameter of the spot contamination was altered. Contamination areas ranged from 0.2 cm² (the smallest assumed size of spot contamination due to nuclear fallout) to 25 cm². In each simulation, the spot of contamination was centered at the same location on the center of the phantom's left forearm. In addition to the spot contamination simulations, a final simulation was run in which the entire forearm was contaminated. In all simulations, the contamination was modeled to be uniformly distributed within the designated area.

3.4.5 Variation in Exposure Time

Monte Carlo simulations of each radionuclide examined were used to obtain the initial dose rate from the contamination as described in Section 3.5. For each of these simulations, a

0.2 cm² spot of contamination was present, the detector probe was modeled to be 1 cm away from the contaminated surface, the epidermis was modeled to be 70 μ m thick, and the activity present was such that it elicited a detector response of 1000 cpm. The total dose to the dermis was calculated for each radionuclide for exposure times of 12 hours, 24 hours, 36 hours, and 14 days as

$$D = \dot{D}_0 \int e^{-\lambda t} dt$$

where \dot{D}_0 is the initial dose rate as calculated from the Monte Carlo simulation, λ is the physical decay constant of the corresponding isotope, and t is the exposure time.

3.5 Relationship Between Dose and Detector Response

In each simulation, two tallies were calculated. The first was a pulse height tally, which provides the energy distribution of the pulses created in the GM. Bloch et al. found that for the fill gas mixture and pressure used, a minimum of 1.6 keV must be deposited in the gas to create a pulse. Therefore, the pulse height tally was binned and the portion of the tally below 1.6 keV was discarded. The integrated remainder of the tally provides the efficiency to the detector for the geometry and source used in that simulation.

The amount of activity assumed to be present was such that it elicited a detector response of 1000 counts per minute (cpm). The activity (dpm) required to produce the assumed count rate was determined as

$$A = \frac{1000cpm}{\varepsilon_{calculated}}$$

where $\varepsilon_{calculated}$ is the detection efficiency calculated in the Monte Carlo simulation.

A dose volume was defined as a 10 cm² area centered at the site of the contamination and extending from the boundary between the epidermis and dermis to the maximum depth of the dermis. The mass of this volume was calculated with an MCNP simulation. An energy deposition tally (MeV per source particle) was calculated over the defined dose volume. The volume averaged dose rate to the dermis was calculated as

$$\dot{D} = \frac{A \times (E/n) \times (1.602 \times 10^{-13})}{m}$$

where A is the calculated activity in dpm, (E/n) is the average energy deposited per particle in MeV/s.p., and m is the mass of the defined dose volume in kg.

CHAPTER 4

RESULTS

4.1 Pancake Probe Model Verification

The original gamma activity of the Cs-137 source used for the verification measurements was $1.14 \pm 0.057 \mu\text{Ci}$ with an assay date of September 26, 1988. At the time of the measurements, the activity of the sealed Cs-137 source had decayed to $0.58 \pm 0.03 \mu\text{Ci}$. The average detector reading was 2086 ± 180 cpm. Therefore, the efficiency of the pancake probe was experimentally found to be $0.16 \pm 0.016 \%$ for Cs-137 gamma radiation. The Monte Carlo model determined the efficiency of the pancake probe to be $0.1204 \pm 0.0003 \%$ for Cs-137 gamma radiation.

The original activity of the Tc-99 source used to experimentally validate the pancake probe model was $0.00558 \pm 0.000279 \mu\text{Ci}$ on its assay date of October 10, 1988. At the time the measurements were taken, the activity of the source remained approximately $0.00558 \mu\text{Ci}$. The average detector reading was 1542.5 ± 169 cpm. Therefore, the experimentally determined efficiency of the pancake probe for Tc-99 was $12 \pm 1.5 \%$. The Monte Carlo model calculated the detection efficiency to be $15.157 \pm 0.002 \%$ for Tc-99 beta radiation.

Four factors may have contributed to the error into this simulation. First, statistical error was introduced by both the experimental decay and the Monte Carlo methods. Second, several of the experimental materials are protected as proprietary information. Assumptions had to be made regarding the composition of such materials for the Monte Carlo models. Energy deposition and scattering is dependent on material composition; therefore, incorrectly defined materials could introduce large error in the simulated detection efficiency. Similarly, error was introduced by simplifications in the MCNP model. The sources were modeled in air as opposed to on the bench top on which the measurements were taken. The

geometry of the plastic section of the source tray was also simplified. These simplifications could reduce the amount of scatter which reaches the detector. Finally, some error may have been introduced by the model's imperfect beta spectrum representation. While experimentally a beta spectrum is a continuous probability function, the energy of each source particle in the MCNP model is sampled from a histogram of beta energies probabilities.

4.2 Variation Associated with Epidermal Thickness

There was no statistically significant change in detection efficiency with increased epidermal thickness as can be seen in Figure 4.1. This was expected as neither factors attributing to the intrinsic detection efficiency nor the geometric detection efficiency were altered.

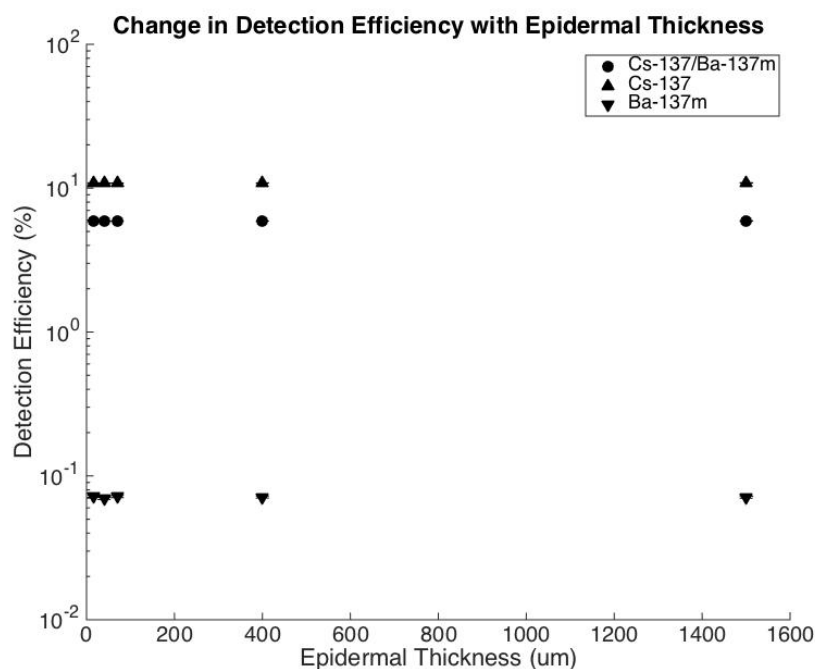


Figure 4.1: Change in Cs-137/Ba-137m beta detection efficiency, gamma detection efficiency, and total detection efficiency with respect to epidermal thickness

The energy imparted per decay to the defined dose volume for the five simulated epidermal thicknesses are displayed in Table 4.1. As can be seen in Figure 4.2, the energy imparted decreased approximately exponentially with increasing epidermal thickness. As

the thickness of the epidermis increases, the more energy beta particles will deposit in the epidermis before reaching the dermis. Only the most energetic beta particles will have enough energy to penetrate the epidermis. Those that do manage to reach the dermis will have less energy to deposit in the viable cells than they would with a thinner epidermis. Similarly, gamma-rays will be exponentially attenuated as they travel through the epidermis. The thicker the epidermis is, the greater the number of gamma-rays that will interact while passing through it. However, variations in the thickness of the epidermis affect the energy deposited by beta particles and electrons to a greater extent than the energy deposited by gamma-rays.

Table 4.1: Energy deposited per decay vs. epidermal thickness for Cs-137/Ba-137m skin contamination

Epidermal Thickness (μm)	Energy Imparted per Decay (keV)
17	75.66 ± 0.08
40	67.13 ± 0.08
70	58.79 ± 0.07
400	19.46 ± 0.03
1500	4.50 ± 0.014

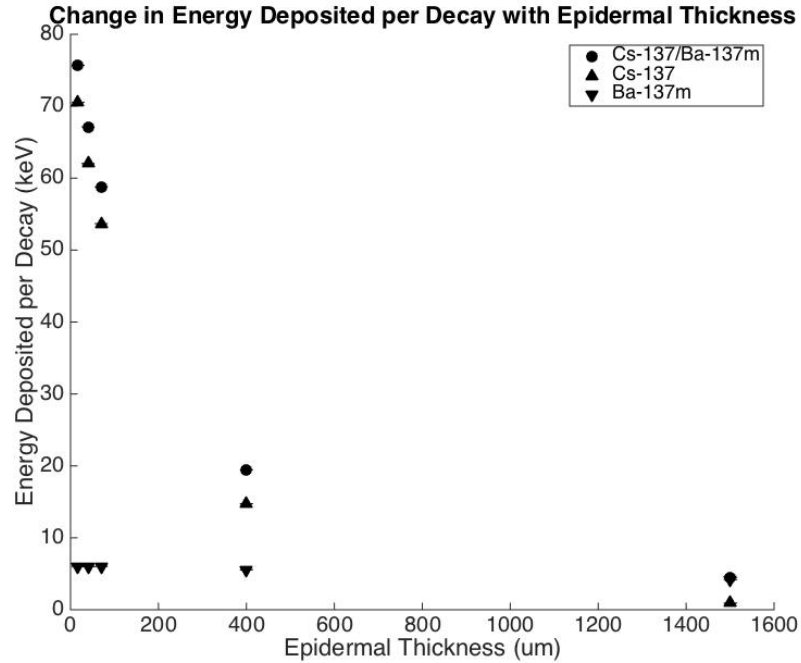


Figure 4.2: Energy deposited in the dermis per decay from Cs-137/Ba-137m skin contamination as a function of epidermal thickness.

The decrease in energy imparted to the dermis with increasing epidermal thickness drives the relationship between the dose rate to the dermis and the detector response. As such, the dose rate decreases approximately exponentially with increasing epidermal thickness, as seen in Figure 4.3. The data markers in Figure 4.3 are larger than the stated uncertainty. Table 4.2 presents the dose rate for epidermal thicknesses of 17 μm , 40 μm , 70 μm , 400 μm , 1500 μm assuming that the activity is such that it would elicit a detector response of 1000 cpm.

Table 4.2: Dose rate to the dermis vs. epidermal thickness for Cs-137/Ba-137m skin contamination

Epidermal Thickness (μm)	Dose Rate ($\mu\text{Gy/hr}$)
17	5.55 ± 0.01
40	4.930 ± 0.009
70	4.315 ± 0.008
400	1.427 ± 0.003
1500	0.3311 ± 0.0006

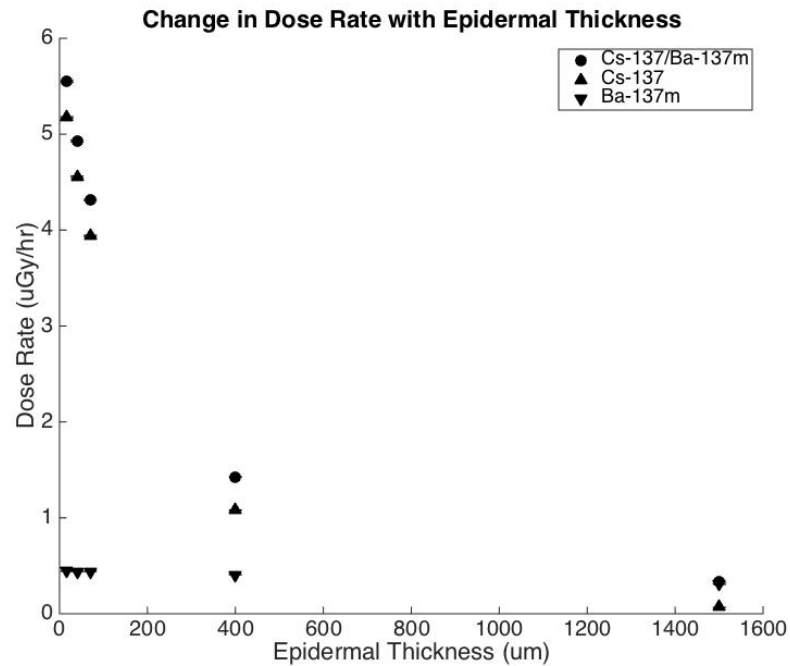


Figure 4.3: Average dose rate to the dermis from Cs-137/Ba-137m skin contamination eliciting a 1000 cpm detector response as a function of epidermal thickness

Applying a decontamination screening criteria developed under the assumption that the epidermis is 70 μm to screening an individual's trunk (approximately 40 μm) would lead to an underestimation of the dose by only approximately 12%. However, applying such

a screening criteria to the face could lead to an underestimation of as much as 22% and applying the criteria to the fingers and the soles of the feet (approximately 1500 μm) would lead to an overestimation of up to approximately 202% and 1203%, respectively. This overestimation could lead to the allocation of time and resources to the decontamination of individuals whom are not at risk for adverse effects. In setting a screening criteria, one should also remember that the depth of the epidermis is not uniform within the same body site or from one individual to the next.

4.3 Variation Associated with Radionuclide Present

The detection efficiencies for Tc-99, I-131, Cs-137, Cs-137/Ba-137m, Sr-90, Y-90, and Sr/Y-90 are tabulated in Table 4.3 and depicted graphically in Figure 4.4. The data markers in Figure 4.4 are larger than the stated uncertainty.

As expected, the detection efficiency was dependent on the isotopes present in the contamination. At low energies, the detection efficiency of beta particles increases with energy. As the energy increases, it becomes more probable that the beta particle will pass through the detector window into the active volume. However, as the energy continues to increase, the particle's LET decreases. As the probability of the particle depositing enough energy in the active volume to create a detectable pulse decreases, the intrinsic efficiency decreases. This can be seen in the Y-90 detection efficiency.

Also as expected, a drop in the detection efficiency is seen in the Cs-137/Ba-137m as compared to Cs-137 due to the low detection efficiency of gamma-rays. In this simulation, the detection efficiency of the Ba-137m gamma-rays was $0.06976 \pm 0.000012\%$. Therefore, the detection efficiency of Cs-137 is cut nearly in half with the addition of its Ba-137m progeny.

Table 4.3: Detection efficiency vs. contamination radionuclides

Radionuclide	Mean Beta Energy (keV)	Detection Efficiency (%)
Tc-99	101.2	9.80 ± 0.02
I-131	181.8	10.72 ± 0.014
Cs-137	188.3	10.85 ± 0.02
Cs-137/Ba-137m	188.3	5.90 ± 0.011
Sr-90	195.9	11.06 ± 0.02
Y-90	932.7	9.74 ± 0.02
Sr/Y-90	564.3	10.40 ± 0.02

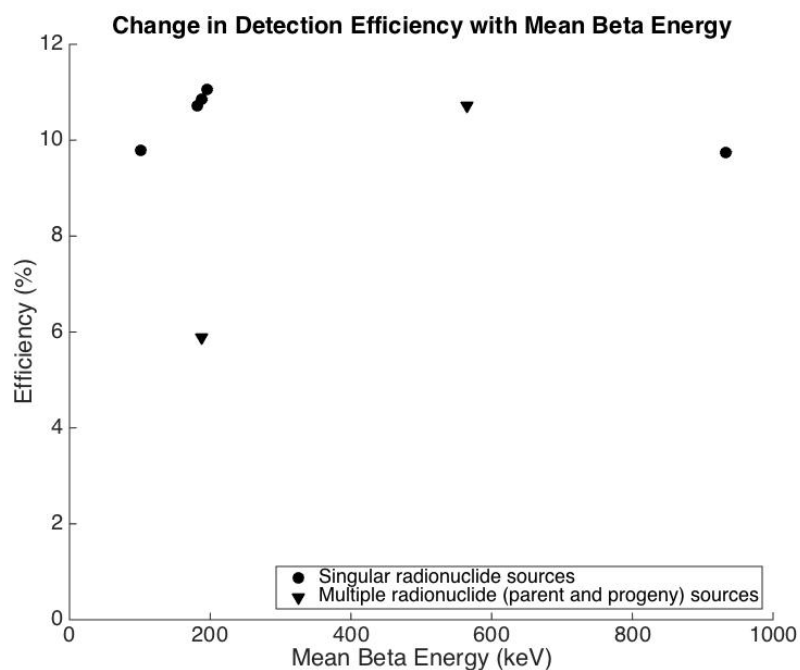


Figure 4.4: Change in detection efficiency with respect to radionuclides present

The energy imparted to the dermis per decay for Tc-99, I-131, Cs-137, Cs-137/Ba-137m, Sr-90, Y-90, and Sr/Y-90 is tabulated in Table 4.4 and depicted graphically in Figure

4.5. The data markers in Figure 4.5 are larger than the reported error. The energy imparted to the dermis per particle was dependent on the isotopes present in the contamination. This result was anticipated. The greater the beta energy, the greater the probability that the beta particle will penetrate the epidermal layer and deposit its energy in the dermis. As can be seen in Figure 4.5, the Cs-137/Ba-137m and Sr/Y-90 sources depart from this trend. While Tc-99, I-131, Cs-137, Sr-90, and Y-90 each emit one particle per decay, an increase in the energy imparted per decay is seen for the Cs-137/Ba-137m and Sr/Y-90 sources due to each emitting an average of more than one particle per decay.

Table 4.4: Energy deposition per particle vs. contamination radionuclides

Radionuclide	Mean Beta Energy (keV)	Energy Deposition per Particle
Tc-99	101.2	15.67 ± 0.02
I-131	181.8	47.67 ± 0.03
Cs-137	188.3	53.7 ± 0.07
Cs-137/Ba-137m	188.3	58.69 ± 0.07
Sr-90	195.9	52.4 ± 0.04
Y-90	932.7	262.1 ± 0.2
Sr/Y-90	564.3	314.5 ± 0.2

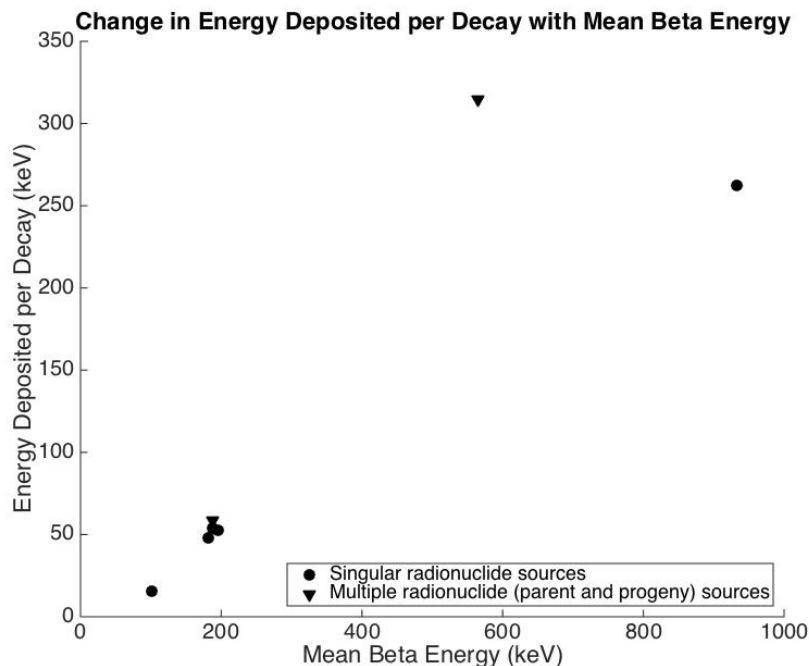


Figure 4.5: Change in energy deposition with respect to radionuclides present

Table 4.5 presents the dose rate for Tc-99, I-131, Cs-137, Cs-137/Ba-137m, Sr-90, Y-90, and Sr/Y-90 spot contamination of the skin assuming that the activity present is such that a detector response of 1000 cpm would be elicited. This result is depicted graphically in Figure 4.6. The data markers in Figure 4.6 are larger than the reported error. As one can see, an increase in energy of the beta particle corresponds to an increase in dose rate in the dermis. Again, a departure from this trend is seen in the Cs-137/Ba-137m and Sr/Y-90 sources. The increase in the dose rate from Sr/Y-90 as compared to the trend is due to the two particle emissions for every decay. The increase in dose rate from Cs-137/Ba-137m as compared to the trend is due to two factors. First, the previously mentioned decreased efficiency due to the gamma-rays increases the amount of activity required to elicit a 1000 cpm response. Second, similarly to Sr/Y-90, on average, 1.85 particles are emitted per decay, increasing the energy deposited. Both of these factors increase the dose rate.

Table 4.5: Dose rate to the dermis from skin contamination corresponding to a 1000 cpm detector response vs. contamination radionuclides

Radionuclide	Mean Beta Energy (keV)	Dose Rate ($\mu\text{Gy/hr}$)
Tc-99	101.2	0.692 ± 0.0012
I-131	181.8	1.924 ± 0.003
Cs-137	188.3	2.139 ± 0.004
Cs-137/Ba-137m	188.3	4.305 ± 0.008
Sr-90	195.9	2.050 ± 0.004
Y-90	932.7	11.64 ± 0.03
Sr/Y-90	564.3	12.70 ± 0.02

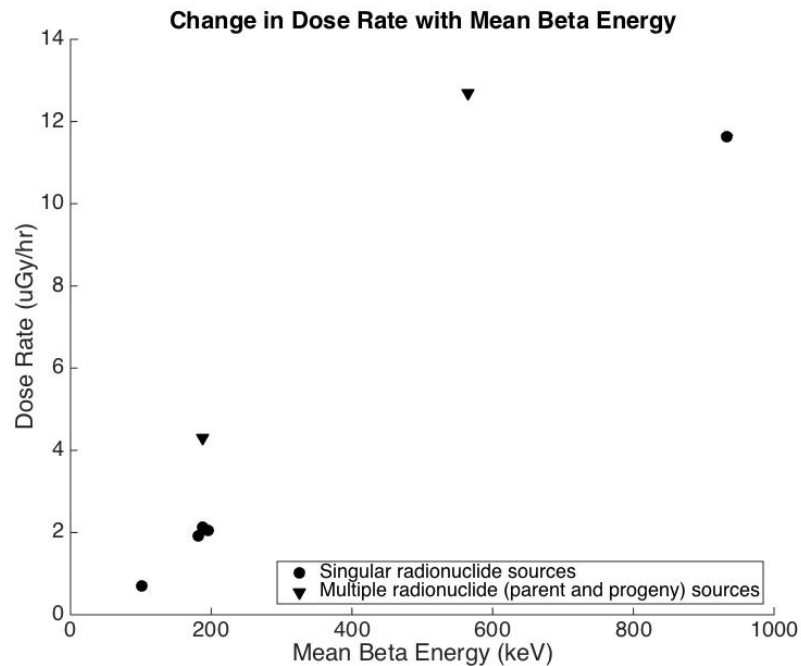


Figure 4.6: Average dose rate to the dermis from skin contamination eliciting a 1000 cpm detector response with respect to radionuclides present

If a screening criteria developed around Cs-137/Ba-137m contamination were applied

for an incident involving Sr/Y-90, a contaminated individual would receive approximately three times the anticipated skin dose for a given detector reading. Similarly, if one were to use such a screening criteria in a Tc-99 incident, time and resources would be applied to decontaminating individuals who would only receive approximately one sixth of the anticipated skin dose for a given detector reading.

4.4 Variation Associated with Source-to-Detector Distance

The results examining the variation of detection efficiency with change in separation between the detector probe and the contaminated skin surface are tabulated in Table 4.6 and displayed graphically in Figure 4.7. The data markers used in Figure 4.7 are larger than the reported error. As expected, the detection efficiency decreased with increasing separation between the contaminated surface and the detector probe. Although the overall detection efficiency for the Ba-137m gamma-rays is lower than the detection efficiency of the Cs-137 beta particles, the variation in separation between the detector probe and the contaminated surface affects the detection efficiency of the beta particles and gamma-rays to a similar extent in the range of distances studied.

Table 4.6: Detection efficiency of Cs-137/Ba-137m skin contamination vs. source-to-detector distance

Separation (cm)	Detection Efficiency (%)
1	5.90 ± 0.011
2	3.421 ± 0.009
2.54	2.627 ± 0.008
5.08	0.948 ± 0.005
7.62	0.453 ± 0.003

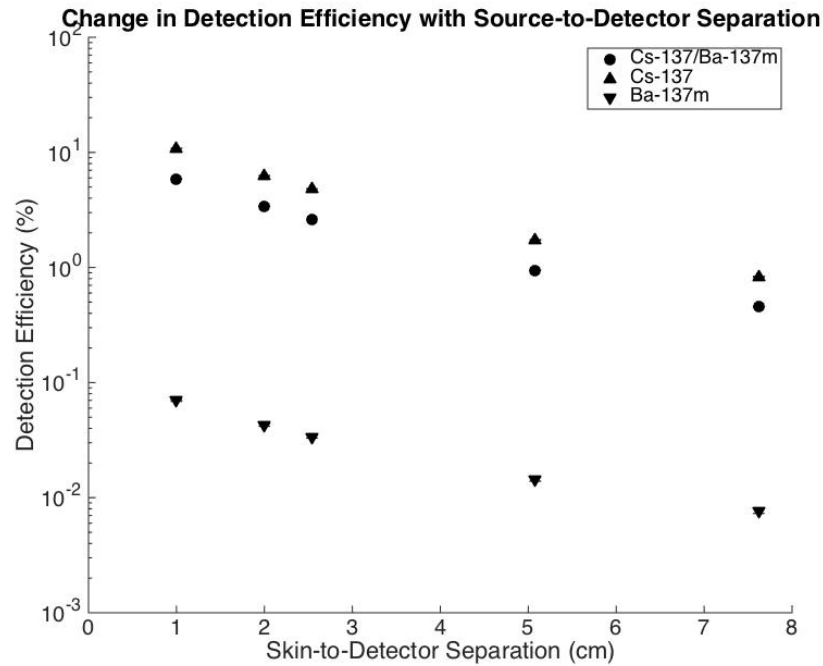


Figure 4.7: Change in Cs-137/Ba-137m beta detection efficiency, gamma detection efficiency, and total detection efficiency with respect to source-to-detector distance

As anticipated, there was no statistically significant change in the energy imparted to the dermis with respect to the separation between the contaminated surface and the detector probe, as can be seen in Figure 4.8.

Table 4.7: Energy imparted per decay vs. source-to-detector distance for Cs-137/Ba-137m skin contamination

Separation (cm)	Energy Imparted (keV/s.p.)
1	58.69 ± 0.07
2	58.48 ± 0.07
2.54	58.43 ± 0.07
5.08	58.34 ± 0.07
7.62	58.33 ± 0.07

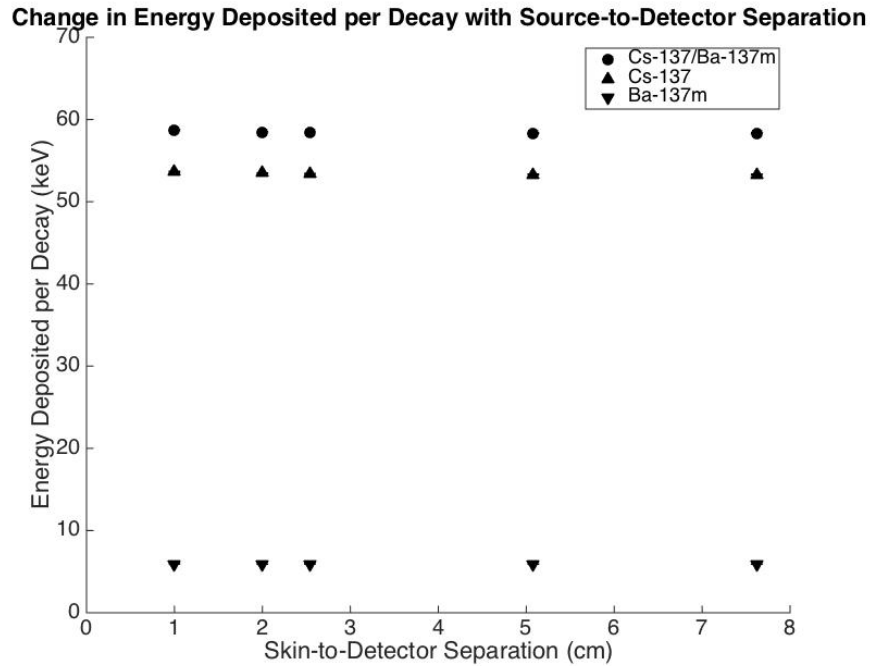


Figure 4.8: Change in average energy deposited in the dermis from Cs-137/Ba-137m skin contamination with respect to source-to-detector distance

Therefore, for a set detector response, an increase of dose rate with increasing separation between the contaminated surface and the detector probe was observed. The dose rate for separations of 1 cm, 2 cm, 1", 2", and 3" is tabulated in Table 4.8 and displayed in Figure 4.9. The data markers used in Figure 4.9 are larger than the reported error. These dose rates assume a detector response of 1000 cpm from Cs-137/Ba-137m contamination. Similarly to the efficiency, although the overall dose rate from the Ba-137m gamma-rays is lower than the dose rate from the Cs-137 beta particles, the variation in separation between the detector probe and the contaminated surface affects the dose rate from the beta particles and gamma-rays to a similar extent.

Table 4.8: Dose rate vs. source-to-detector distance for Cs-137/Ba-137m skin contamination

Separation (cm)	Dose Rate ($\mu\text{Gy/hr}$)
1	4.305 ± 0.008
2	7.40 ± 0.02
2.54	9.62 ± 0.03
5.08	26.6 ± 0.2
7.62	55.7 ± 0.4

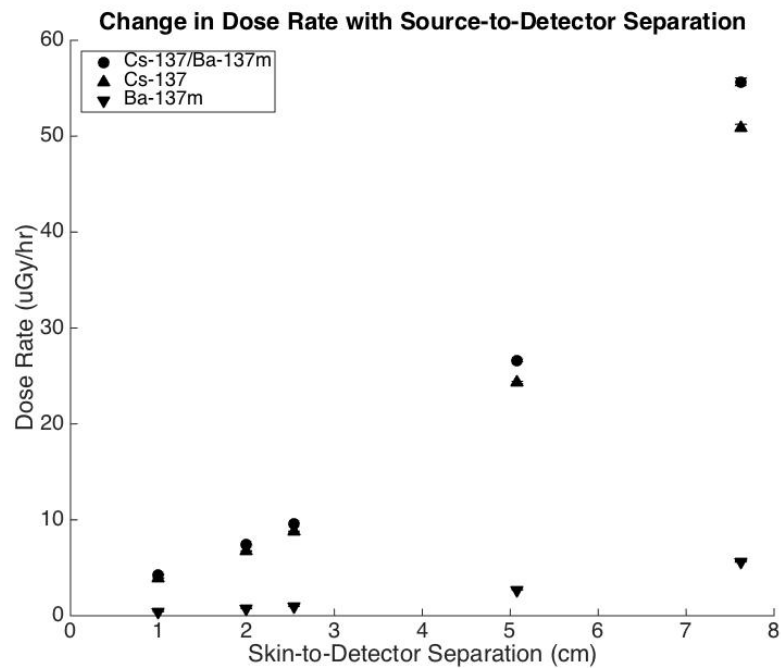


Figure 4.9: Average dose rate to the dermis from Cs-137/Ba-137m skin contamination eliciting a 1000 cpm detector response with respect to source-to-detector distance

It should be noted that a separation of 2" or 3" is not recommended; however it is often observed and, therefore, must be accounted for. For Cs-137/Ba-137m contamination, in the event a screening criteria designed utilizing a 1 cm separation between the probe

and skin surface is applied to an individual screened with a separation of 2", the dose received by that individual will be underestimated by approximately 520%. If that individual is screened with a separation of 3", the dose received by that individual will be underestimated by approximately 1200%. Even among the proper screening techniques, a large error can be introduced due to variation in the separation between the detector probe and the contaminated skin surface. Screening with a separation of 1" while using a screening criteria designed with a separation of 1 cm will underestimate the dose by approximately 120%. Similarly, screening an individual with a separation of 1 cm while using a screening criteria designed with a separation of 1" will overestimate the dose by approximately 55% possibly leading to time and resources being allocated to decontaminating individuals who are below the screening criteria.

4.5 Variation Associated with Extent of Contamination

The Monte Carlo calculated detection efficiency for various contamination areas is presented in Table 4.9. As can be seen graphically in Figure 4.10, the detection efficiency decreases linearly with increasing contamination area. This is anticipated as the geometric efficiency decreases as the contamination area grows.

Table 4.9: Detection efficiency of Cs-137/Ba-137m skin contamination for a pancake GM probe with a 15 cm² window vs. contamination area

Contamination Area (cm ²)	Detection Efficiency (%)
0.2	5.90 ± 0.011
1	5.83 ± 0.011
2	5.73 ± 0.011
4	5.58 ± 0.011
6	5.37 ± 0.011
8	5.208 ± 0.008
10	5.07 ± 0.010
12	4.90 ± 0.010
14	4.74 ± 0.010
16	4.59 ± 0.010
18	4.44 ± 0.010
20	4.287 ± 0.009
25	3.922 ± 0.009

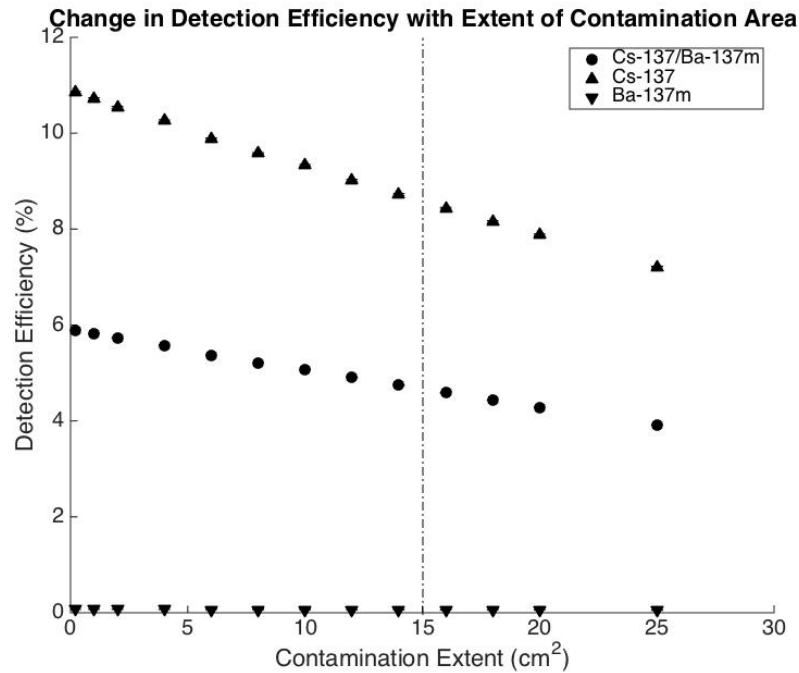


Figure 4.10: Change in Cs-137/Ba-137m beta detection efficiency, gamma detection efficiency, and total detection efficiency with respect to extent of contamination. The area of the detector window (15 cm²) is indicated with the vertical dotted line.

The energy imparted to the dermis per particle is tabulated in Table 4.10. As can be seen in Figure 4.11, the energy imparted per particle remains stable for small contamination areas. As the contamination area approaches the size of the dose volume, the energy imparted per particle begins to decrease. This is expected as beta particles created in the periphery of the contamination area begin to scatter out of or never reach the dose volume before depositing all of their energy.

Table 4.10: Energy imparted per decay vs. contamination area for Cs-137/Ba-137m skin contamination

Contamination Area (cm ²)	Energy Imparted per Particle (keV)
0.2	58.69 ± 0.07
1	58.65 ± 0.07
2	58.51 ± 0.07
4	58.50 ± 0.07
6	58.33 ± 0.07
8	58.24 ± 0.07
10	57.78 ± 0.07
12	50.22 ± 0.07
14	43.25 ± 0.06
16	37.98 ± 0.06
18	33.86 ± 0.06
20	30.48 ± 0.05
25	24.42 ± 0.05

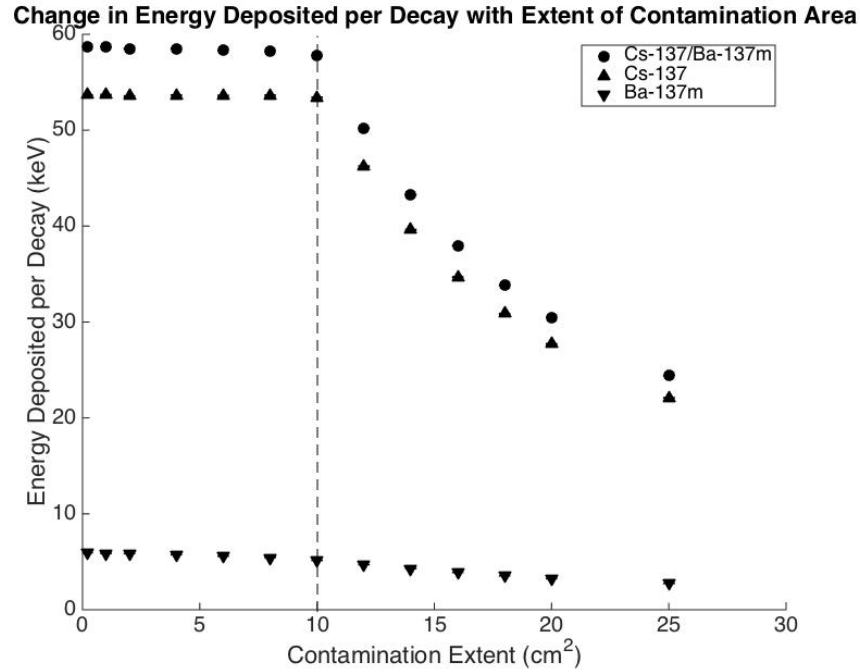


Figure 4.11: Change in energy imparted per decay from Cs-137/Ba-137m skin contamination with respect to extent of contamination. The vertical dashed line represents the area of the defined dose volume (10 cm²).

The calculated dose rates with respect to extent of contamination are presented in Table 4.11. As can be seen in Figure 4.12, the dose rate increases with contamination area until a maximum dose rate is reached at approximately 10 cm², the area of the dose volume. At points within this boundary, although the energy imparted per particle is decreasing, it remains relatively steady as compared to the detection efficiency. Therefore, the dose rate is driven by its inverse proportionality to the detection efficiency. Beyond this boundary, the dose rate decreases dramatically. This is expected as at this distance, electrons created in the periphery of the contamination area no longer contribute dose to the defined dose volume.

Table 4.11: Dose rate vs. contamination area for Cs-137/Ba-137m skin contamination

Contamination Area (cm ²)	Dose Rate (μ Gy/hr)
0.2	4.305 ± 0.008
1	4.355 ± 0.008
2	4.416 ± 0.008
4	4.538 ± 0.009
6	4.698 ± 0.009
8	4.838 ± 0.008
10	4.93 ± 0.010
12	4.431 ± 0.009
14	3.945 ± 0.008
16	3.582 ± 0.008
18	3.302 ± 0.007
20	3.076 ± 0.007
25	2.693 ± 0.006

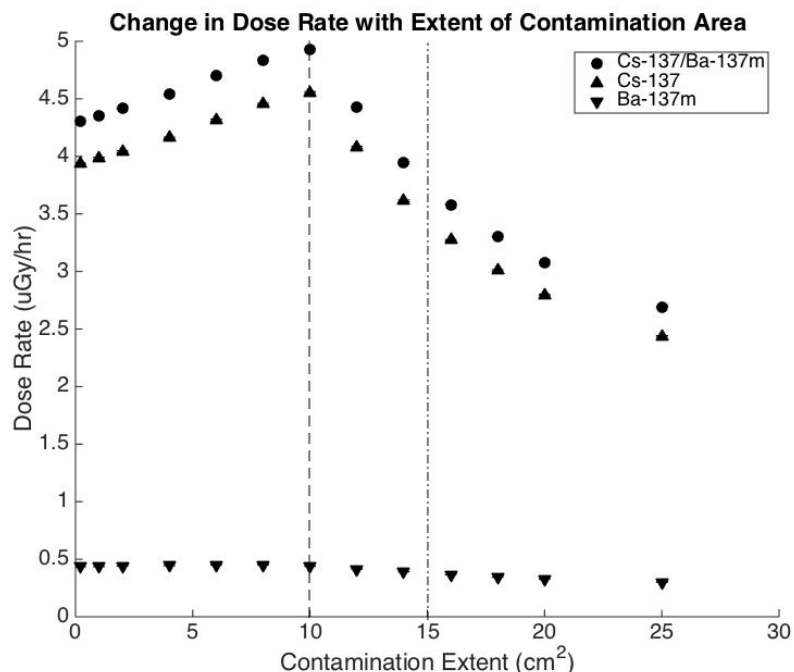


Figure 4.12: Average dose rate to the dermis from Cs-137/Ba-137m skin contamination eliciting a 1000 cpm detector response with respect to extent of contamination. The vertical dashed line represents the area of the defined dose volume (10 cm²). The area of the detector window (15 cm²) is indicated with the vertical dotted line.

It is expected that as the contamination volume continues to grow, the detection efficiency and the energy imparted will begin to decrease at similar rates. This will cause the dose rate to stabilize at a minimum dose rate. For the simulation in which contamination encompasses the entirety of the forearm (widespread contamination), the dose rate was calculated to be $1.88 \pm 0.02 \mu\text{Gy/hr}$. Assuming the dose rate has stabilized at this point, utilizing a screening criteria developed for widespread contamination for spot contamination could lead to underestimation of the absorbed dose by up to a factor of 2.6. This result accounts only for the effects of variation in the extent of contamination on the relationship between the detector response and the dose to the dermis. It does not account for volume effects due to skin repair mechanisms.

4.6 Variation Associated with Exposure Time

The absorbed dose for 12 hour, 24 hour, 36 hour, and 14 day increments for each radionuclide simulated is tabulated in Table 4.12.

Table 4.12: Absorbed dose from Cs-137/Ba-137m skin contamination eliciting a 1000 cpm detector response vs. exposure time

Absorbed Dose ($\mu\text{Gy}/\text{kcpm}$)				
Radionuclide	Exposure Time			
	12 hours	24 hours	36 hours	14 days
Tc-99	8.30 ± 0.01	16.61 ± 0.03	24.92 ± 0.04	232.5 ± 0.4
I-131	22.60 ± 0.03	44.25 ± 0.06	64.98 ± 0.08	375.0 ± 0.5
Cs/Ba-137	51.7 ± 0.10	103.3 ± 0.2	155.0 ± 0.3	1446 ± 3
Sr/Y-90	152.3 ± 0.2	304.7 ± 0.4	457.0 ± 0.7	4264 ± 6

As can be seen graphically in Figure 4.13, the decrease in activity over the exposure time is negligible for Tc-99, Cs-137/Ba-137m, and Sr/Y-90. As such the dose rate remains stable providing an approximately linear relationship between exposure time and absorbed dose. Unlike the other radionuclides, I-131 has a relatively short half-life in comparison to the exposure time. As such, the decrease in activity over a 14 day period is no longer negligible and the linear relationship between exposure time and dose is no longer valid.

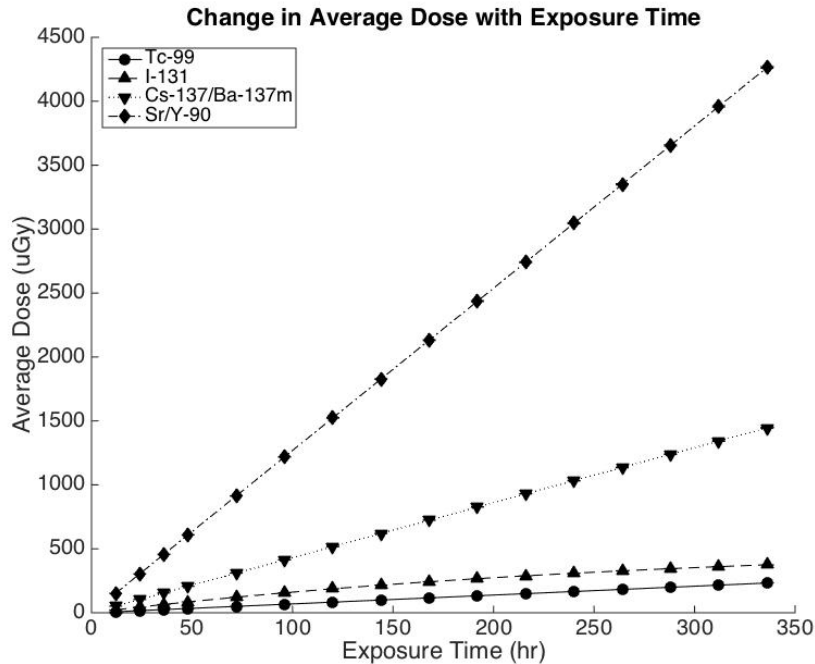


Figure 4.13: Change in absorbed dose to the dermis from skin contamination eliciting a 1000 cpm response at 1 cm with respect to exposure time

Applying a screening criteria developed under the assumption of a 12 hour exposure time to a situation in which there will be a 36 hour exposure time could lead to an underestimation of the dose by a factor of approximately three for each of the four isotopes examined in this study.

4.7 Comparison of Variation in Assumed Factors

In Figure 4.14, the variation in dose rate with respect to each previously discussed factor assuming a detector response of 1000 cpm is shown. Variations in epidermal thickness, contamination radionuclide, and separation between the detector probe and the contaminated surface have an approximately equal relative effect on the relationship between the absorbed dose to the dermis and the detector response. As can be seen by the graph, variation in the separation between the detector probe and the contaminated surface has the greatest absolute effect on the relationship between the absorbed dose to the dermis and

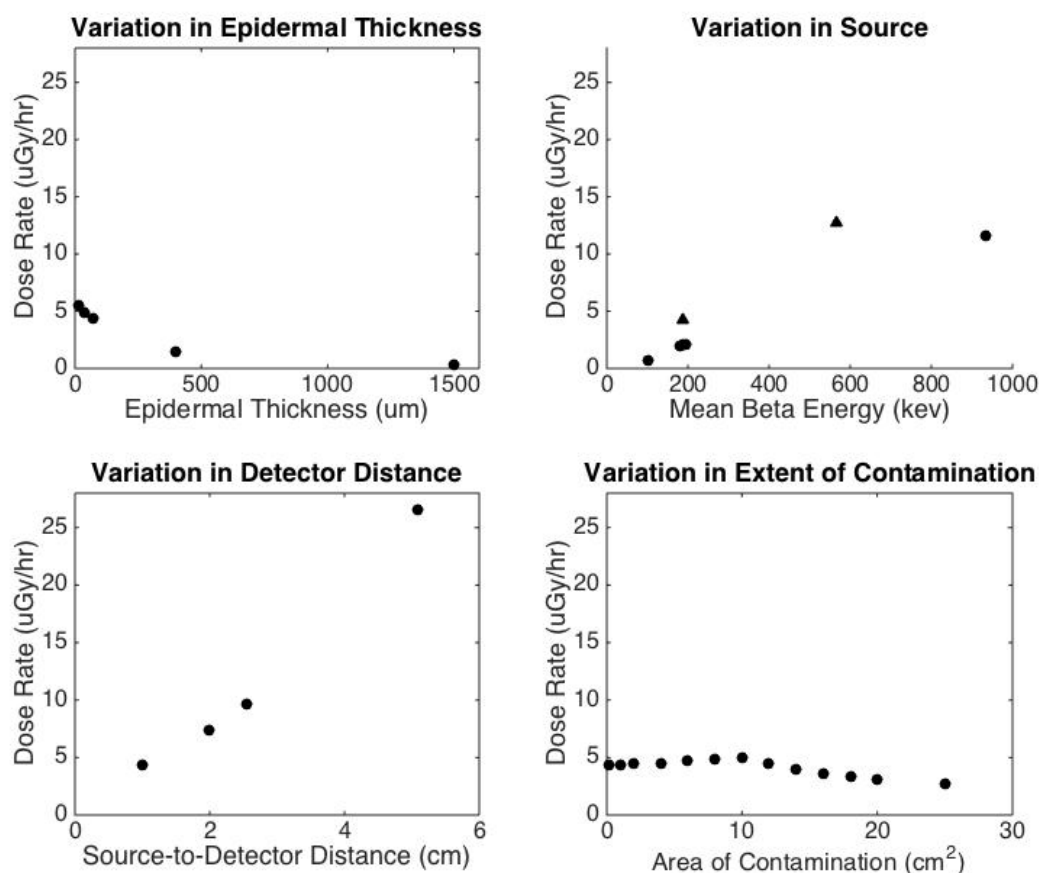


Figure 4.14: Top left: Change in average dose rate to the dermis from Cs-137/Ba-137m skin contamination eliciting a 1000 cpm detector response with respect to epidermal thickness. Bottom left: Change in average dose rate to the dermis from Cs-137/Ba-137m skin contamination eliciting a 1000 cpm detector response with respect to source-to-detector distance. Top right: Change in average dose rate to the dermis from skin contamination eliciting a 1000 cpm detector response with respect to contamination source. Bottom right: Change in average dose rate to the dermis from Cs-137/Ba-137m skin contamination eliciting a 1000 cpm detector response with respect to contamination extent.

the detector response. However, within the range of proper scanning technique, the separation between the probe and the contaminated surface accounts for the least degree of variability in the relationship between detector response and dose to the dermis. Assuming proper scanning technique is applied and accounting for the fact that only a select few radionuclides were examined in this research, variation of the radionuclides involved in the contamination provide the greatest range of variability in the relationship between the

detector response and the absorbed dose to the dermis.

4.8 Comparison of Suggested Screening Criteria

The suggested screening criteria can be compared by applying them all to the same hypothetical incident. Let us assume that an individual with a 0.2 cm^2 spot of loose Cs/Ba-137 contamination is being screened with a pancake probe. We will assume that for each scenario, the spot contains an activity eliciting a detector response equivalent to the screening criteria and that the separation between the probe and contaminated surface used is that dictated by the screening criteria. As the screening criteria suggested by the EPA does not provide a suggested separation between the probe and the contaminated surface, 1" will be assumed. As the screening criteria suggested by the EPA is based on the current background, it will be assumed that the background is elevated to 50 cpm. It will be assumed that 36 hours will pass between the contamination event and the time of decontamination, i.e. the individual will be exposed for a total of 36 hours. The volume averaged absorbed dose to the dermis is presented in Table 4.13 for each screening criteria.

Table 4.13: Absorbed dose from Cs-137/Ba-137m spot contamination with the direct application of suggested generic screening criteria

Guidance Document	Skin-to-Detector Distance (cm)	Screening Criteria	Absorbed Dose (μGy)
FEMA-REP-22 (modern pancake GM)	2.54	10,000 cpm	3460 ± 11
FEMA-REP-22 (CD V-700)	2.54	300 cpm	103.8 ± 0.3
CRCPD Handbook	2.54	10,000 cpm	3460 ± 11
EPA PAG Manual	2.54	$2 \times$ background	17.32 ± 0.015
IAEA EPP-NPR-OILs 2017 (OIL 4_{β})	2	1,000 cps	15980 ± 40
IAEA EPP-NPR-OILs 2017 (OIL 4_{γ})	10	$1 \mu\text{Sv/h}$	3490 ± 30
NCRP Report No. 161	1	$10,000 \text{ Bq/cm}^2$	1097 ± 0.0002
NCRP Report No. 165	1	$600,000 \text{ dpm/cm}^2$	1097 ± 0.0002
NCRP Report No. 166	1	1,000 cpm	155.0 ± 0.3

As can be seen in Table 4.13, the 2017 EPA PAG Manual provides the most conservative screening criteria for spot contamination. However, this result can be misleading as the EPA bases their suggested screening criteria on the present background. As the background increases, the screening criteria suggested by the EPA becomes less conservative. The results in Table 4.13 indicate that IAEA provides the least conservative screening criteria, OIL 4_{β} . For the given situation, OIL 4_{β} leads to a dose approximately 360% higher than the second least conservative criteria, provided by OIL 4_{γ} , FEMA-REP-22, and the CRCPD

Handbook. However, both FEMA-REP-22 and the CRCPD Handbook recommend that the screening criteria be reduced to 1,000 cpm for fixed contamination. In which case the absorbed dose resulting from these criteria would be decreased to 10% of that shown in Table 4.13, further increasing the dose difference. It should also be noted that the dose reported in Table 4.13 corresponding to $OIL4_\gamma$ assumes that there is no beta shield applied to the detector probe. If a beta shield were applied to the detector probe, $OIL4_\gamma$ could lead to a dose of close to 0.5 Gy in this scenario (a dose approximately 3,000% greater than that resulting from $OIL4_\beta$). As it stands, applying the suggested screening criteria to the presented scenario leads to a factor of over 900 between the highest and lowest estimated dose.

CHAPTER 5

CONCLUSION AND FUTURE WORK

This work evaluated the impact of five factors on the relationship between detector response and absorbed dose during a nuclear or radiological emergency. The results indicate that variations in any of the five factors (epidermal thickness, contamination radionuclide, source-to-detector distance, contamination extent, and exposure time) could greatly impact the relationship between the detector response and the skin dose due to external contamination. It is clear that for a given external contamination screening criterion, the resulting skin dose can vary significantly depending on the nature and distribution of contamination on the skin and the survey technique. The application of these results along with future work to emergency planning may aid in adjusting screening levels based on the specific circumstances of the situation at hand.

Only one detector type was evaluated in this work. Several detector options may be available to first responders including EPDs, ion chambers, and other types of GM probes. Future research should expound on these findings to include the evaluation of variation due to characteristics of the contamination and survey techniques with alternate detector types.

Only four isotopes were evaluated as the contaminant in this work. Future work should include the evaluation of several additional isotopes likely to become external contamination in the event of a nuclear or radiological emergency. These isotopes should include alpha emitters in addition to beta and gamma emitters.

Finally, additional factors should be accounted for in choosing an appropriate screening criteria. These factors include accounting for the probability of internalization of external contamination, special populations, and limitation of resources.

Appendices

APPENDIX A

SAMPLE MCNP INPUT FILE

Mathematical FEMALE Phantom model

```

C =====
c 0.2 cm2 spot source on left forearm
c GM 1 cm from left forearm
c =====
c ===== Posture Parameters Angles are in degrees
C ===== Posture Parameters Right shoulder rotation:Theta = 0 Phi = 0
C ===== Posture Parameters Right ellbow rotation:Theta = 0 Phi = 0
C ===== Posture Parameters Left ellbow rotation:Theta = 0 Phi = 0
C ===== Posture Parameters Right hip rotation:Theta = 0 Phi = 0
C ===== Posture Parameters Left knee rotation:Theta = 0 Phi = 0
C ===== Posture Parameters Right knee rotation:Theta = 0 Phi = 0
C ===== Posture Parameters Left shoulder rotation:Theta = 0 Phi = 0
C ===== Posture Parameters Left hip rotation:Theta = 0 Phi = 0
C =====
C ===== The Female model is based on the 15 yr Hermaphrodite
C ===== Phantom model – Prostate, Testes and male genitalia are
C ===== removed
C =====
C
C =====
C ===== Description of Input File =====
C =====
C ===== Cell numbers 1-132 are used to describe the phantom and
C ===== 133 is used to describe surrounding around the phantom, which
C ===== is set to vacuum at the moment.
C ===== Surface numbers 1-338 are used to describe the phantom
C ===== and outside.
C ===== Material number 1-25 are allocated to describe phantom
C ===== materials.
C =====
C ===== Therefore, it is important to use
C ===== Cell Number  $i$  135
C ===== Surface Number  $j$  339
C ===== Material Number  $k$  26
C ===== to define new cells, surfaces, materials when needed for
C ===== modification towards adding new objects.
C ===== When new objects are added, make sure to modify the importance
C ===== cards, which are toward the end of the input file, as well.

```

C =====
C
c =====
c Cell Card
c =====
c
C ===== 1.0 Head and Neck =====
C
C =====
C
C 1.1 The Skin of Head and Neck
C =====
C
1 11 -1.09 ((-8 9):-7)-1 12 (2:4:7:(-6 11))
(5:(-10 11):-12)(-5:7:-4:(-13 85 14)
:(2 -1 -14)) #7 #8 #2
VOL=214.8
C =====
C 1.2 The Cranium
C =====
C
2 2 -1.4 (15 -19 7):(16 -20 17 21 -7):(-20 -17 21 -7)
VOL=284.5
C =====
C 1.3 The Teeth
C =====
C
3 2 -1.4 -22 23 24 -25 -26 VOL=30.2
C =====
C 1.4 The Mandible
C =====
C
4 2 -1.4 (-27 29((28 -24 -26):(30 -21 26 -18)))
VOL=144.8
C =====
C 1.5 Nasal Cavity (The Upper Face Region, Facial skeleton)
C =====
C
5 5 -1.22 -31 25 -21 -26 32 33
C
C remove sphenoid Sinus
(39 40)
C remove ethmoid Sinus
(41 42)
C remove frontal Sinus

(43 44)
C remove maxillary Sinus
(45 46)
C VOL=246.2-3.031080975-2.316809810-6.042866874-21.73095454
VOL=213.0782878

C =====
C 1.7 The Brain

C =====
C
6 6 -1.04 (7 -34):(-7 -35 36) VOL=1310.2

C =====
C 1.8 The eyes

C =====
C Left
7 7 -1.07 -32 VOL=6.2

C Right
8 7 -1.07 -33 VOL=6.2
C =====

C 1.9 Total Sinuses
C =====
C

9 4 -0.001205 (-39:-40:-41:-42:-43:-44:-45:-46)
VOL = 33.12171220

C =====
C 1.13 Pharynx(Skeletal Muscle)

C =====
C Residual Wall

C =====
C
10 13 -1.05 -47 50 12 -49 VOL=9.714754084

C =====
C Contents

C =====
C
11 4 -0.001205 -48 12 -49 VOL=23.165

C =====
C Mucosa Wall

C =====
C
12 13 -1.05 -50 48 12 -49 VOL=5.413245916

C =====
C 1.14 Larynx

C =====
C Residual Wall

C =====

C
 13 8 -1.1 54 -52 53 -5 VOL=2.535894335
 C=====

C Content
 C=====

C
 14 4 -0.001205 -51 53 -5 VOL=3.97
 C=====

C Mucosa Wall
 C=====

C
 15 8 -1.1 51 -54 53 -5 VOL=1.350105665
 C=====

C 1.15 Trachea
 C=====

C Residual Wall
 C=====

C
 16 12 -1.03 58 -55 57 -53 VOL=8.674931010
 C=====

C Content
 C=====

C
 17 4 -0.001205 -56 57 -53 VOL=12.799
 C=====

C Mucosa Wall
 C=====

C
 18 12 -1.03 56 -58 57 -53 VOL=1.899068990
 C=====

C 1.16 Thyroid
 C=====

C
 19 10 -1.05 (339 -5 66 -59 60 -61 -65):
 (-339 -5 66 -59 60 -62 -65):
 (339 67 -66 -59 60 63 -65 (53 : 55)):
 (-339 67 -66 -59 60 64 -65 (53 : 55))
 VOL=11.9
 C=====

C 1.17 Nose
 C=====

C Contents
 C=====

C
 20 4 -0.001205 -68 -69 73 1 -76

C remove Center Tissue
(-74:75) Vol=4.7773

C=====

C Nose Wall

C=====

C

21 13 -1.05 -71 -72 73 1 -76 (-75:69)(74:68)

Vol=6.865

C=====

C 1.18 Oral Cavity (Soft tissue Behind mouth and teeth)

C=====

C

22 12 -1.03 (((-30 29 -21 26 -18)

:(-26 -23 24 -25)

:(-26 -28 -24 29))

((77 78):-24:49)((79 81):80:-29)((82 84):-83:26:28))

Vol=231.616

C

C=====

C 1.19 Salivary Glands

C=====

C Left & Right Parotid

C=====

C

C 51 1 -1.04 (-636 : -641) 531 -565

Vol = 38.462

C

C Left & Right Submandibular

C

C 53 1 -1.04 (-637 : -642) -638 536

Vol = 19.296

C

C Left & Right Sublingual

C

C 55 1 -1.04 (-639 : -643) 640 -533 -535

Vol = 7.692

C

C Total Salivary Glands

C

23 12 -1.03 (((-77 : -78) 24 -49):((-79 : -81) -80 29):

((-82 : -84) 83 -26 -28))

Vol = 65.385

C=====

C 1.20 Muscle Part of head and neck

C=====

C
 24 13 -1.05 (-9:-7) -2 12 (6:-11:-12) (-4:7:-5:-14)
 C
 C remove cranium
 (-15:19:-7)(-16:20:-17:-21:7)(20:17:-21:7)
 C remove teeth
 (22:-23:-24:25:26)
 C remove mandible
 (27:-28:-29:24:26)(27:-30:-29:21:-26:18)
 C remove nasal cavity
 (31:-25:21:26:-32:-33)
 C remove spine in the Head and Neck
 (85:89:-88)
 C remove brain
 (-7:34)(7:35:-36)
 C remove eyes
 (32 33)
 C remove larynx
 (52:-53:5)
 C remove trachea
 (55:-57:53)
 C remove pharynx
 (47:-12:49)
 C remove thyroid
 #19
 C remove Oral Cavity
 #22
 C remove salivary glands
 #23
 VOL = 1119.939

C=====

C

C===== 2.0 Skeleton Region =====

C

C=====

C 2.1 Spine

C=====

C 2.1.1 Cervical Verterbra - CV(upper)

C=====

C

25 2 -1.4 -85 -89 88 VOL=130.626

C=====

C 2.1.2 Thoracic Verterbra - TV (middle)

C=====

C

26 2 -1.4 -85 -88 87 VOL=418.90

C=====

C 2.1.3 Lumber Vertebra - LV (lower)

C=====

C

27 2 -1.4 -85 -87 86 VOL=157.258

C=====

C 2.2 Ribs

C=====

C all ribs

28 2 -1.4 91 -90 ((93 -92):(95 -94):(97 -96):(99 -98):

(101 -100):(103 -102):(105 -104):(107 -106):(109 -108):

(111 -110):(113 -112):(115 -114))

VOL=531

C=====

C 2.3 Clavicles

C=====

C both

29 2 -1.4 -116 ((117 -119):(-118 120)) VOL=41.6

C=====

C 2.4 Scapulae

C=====

C both

30 2 -1.4 90 -121 126 -127 ((122 -124):(-123 125))

VOL=154

C=====

C 2.5 Pelvis

C=====

31 2 -1.4 128 -129 130 341 -132 (133:-131)

VOL=460

C

C=====

C

C=====

C

C===== 3.0 Upper Chest Organs =====

C

C=====

C 3.1 Main Bronchi

C=====

C Residual Wall

C=====

C

32 12 -1.03 (152 -144 -146 147 154 -57 339):(-148 153 -150 151 155 -57 -339)

VOL = 9.827

C =====
C Contents
C =====
33 4 -0.001205 (-145 -146 147 154 -57 339):(-149 -150 151 155 -57 -339)
VOL = 10.82584
C =====
C Mucosa Wall
C =====
34 12 -1.03 (145 -152 -146 147 154 -57 339):(-153 149 -150 151 155 -57 -339)
VOL = 2.403
C =====
C 3.2 Lungs
C =====
C left
35 14 -0.26 -154 156 (163:162:161) VOL=1020
C right
36 14 -0.26 -155 156 (-159:160:158:-157) VOL=1180
C =====
C 3.3 Thymus
C =====
37 12 -1.03 -164 VOL=32.725
C =====
C 3.4 Heart
C =====
C
C Wall of heart
C =====
38 15 -1.05 (165 ((-166 168 -167):(170 -169))):
(-165 ((-166 176 -175):(166 172 -171):(-166 -173 174)))
VOL=231
C
C =====
C Contents of heart
C =====
39 15 -1.05 (165 ((-166 -168 169):(-170))):
(-165 ((-166 -176 173):(166 -172):(-166 -174)))
VOL=334
C
C =====
C
C ===== 4.0 Middle Chest Organs =====
C
C =====
C 4.1 Adrenals
C =====

C left
 40 12 -1.03 179 -177 VOL=5.05
 C right
 41 12 -1.03 179 -178 VOL=5.05
 C =====
 C 4.2 Kidneys
 C =====
 C left kidney
 C
 42 16 -1.04 (-180 182) VOL=119.2
 C right kidney
 C
 43 16 -1.04 (-181 -183) VOL=119.2
 C =====
 C 4.3 Liver
 C =====
 44 17 -1.05 -204 -205 207 -206 VOL=1350
 C
 C =====
 C 4.4 Gall bladder
 C =====
 C wall
 45 12 -1.03 (-212 208 -209):(212 -213 210 -211)
 VOL=7.61609
 C contents
 46 12 -1.03 (-212 -208):(212 -210 -213) VOL=47.1
 C
 C =====
 C 4.5 Pancreas
 C =====
 47 18 -1.04 -214 215 (216:-217) VOL=98.929
 C
 C =====
 C 4.6 Spleen
 C =====
 48 19 -1.06 -218 VOL=119
 C
 C =====
 C
 C ===== 5.0 Gastrointestinal tract and contents =====
 C
 C =====
 C 5.1 Male Esophagus /*** 1996 ORNL C&E ***/
 C =====
 C Mucosa Wall of the thoracic portion

C =====
C
49 12 -1.03 (-220 222 206 -88)
VOL = 5.13853867
C =====
C Mucosa Wall of the abdominal portion
C =====
50 12 -1.03 (-219 224 -225)
VOL = .1088341717
C =====
C Remainder Wall of the thoracic and abdominal portion
C =====
51 12 -1.03 (-221 220 206 -88);(-223 219 224 -225)
VOL= 26.4836
C =====
C Contents of the thoracic portion
C =====
52 4 -0.001205 -222 206 -88 VOL=7.065490673
C =====
C
C ===== 5.2 Stomach =====
C
C =====
C Mucosa Wall
C =====
53 20 -1.03 -226 228 VOL=39.3811276
C =====
C Remainder Wall
C =====
54 20 -1.03 -227 226 VOL=73.6188724
C =====
C Contents
C =====
55 20 -1.03 -228 VOL=187
C =====
C
C ===== 5.3 S. intestine =====
C
C =====
56 20 -1.03 -128 230 -231 232 -207
C
C remove a. colon
(235:238:-232)
C remove t. colon
(240:242:-243)

C remove d. colon
(245:238:-232)
VOL=806

C

C=====

C 5.4 Right colon *

C=====

C 5.4.1 A. colon

C Mucosa Wall

C

57 20 -1.03 (-234 236 237 -238) VOL = 16.90747038

C=====

C Remainder Wall

58 20 -1.03 (-235 234 237 -238) VOL = 52.59252962

C=====

C Contents

59 20 -1.03 (-236 237 -238) VOL = 73.4

C=====

C

C 5.4.2 Proximal T. colon

C

C Mucosa Wall

C=====

60 20 -1.03 -239 241 -242 243 -339 VOL = 11.33146720

C=====

C Remainder Wall

C=====

61 20 -1.03 -240 239 -242 243 -339 VOL = 34.81853280

C=====

C Contents

C=====

62 20 -1.03 -241 -242 243 -339 VOL = 48

C=====

C

C 5.5 Left colon

C 5.5.1 Distal T. colon

C

C Mucosa Wall

C=====

63 20 -1.03 -239 241 -242 243 339 VOL = 11.33146720

C=====

C Remainder Wall

C=====

64 20 -1.03 -240 239 -242 243 339 VOL = 34.81853280

C=====

C Contents

C=====

65 20 -1.03 -241 -242 243 339 VOL = 48

C=====

C 5.5.2 D. colon *

C=====

C Mucosa Wall

C=====

66 20 -1.03 (-244 246 247 -238) VOL = 16.69746766

C=====

C Remainder Wall

C=====

67 20 -1.03 (-245 244 247 -238) VOL = 49.79253234

C=====

C Contents

C=====

68 20 -1.03 (-246 247 -238) VOL = 58.93

C

C=====

C 5.6 Rectosigmoid *

C=====

C

C 5.6.1 Sigmoid colon

C=====

C Mucosa Wall

C=====

69 20 -1.03 (-248 251 247):(-249 253 -247)

VOL = 9.098855

C=====

C Remainder Wall

C=====

70 20 -1.03 (-250 248 247):(-252 249 -247)

VOL = 28.306145

C=====

C Total contents

C=====

71 20 -1.03 (-251 247):(-253 -247) VOL = 37.484

C=====

C

C 5.6.2 Rectum

C=====

C Mucosa Wall

C=====

72 20 -1.03 -255 257 -247 341 VOL = 3.85355434

C=====

C Remainer Wall

C=====

73 20 -1.03 -256 255 -247 341 VOL = 10.92644566

C=====

C Contents

C=====

74 4 -0.001205 -257 -247 341 VOL = 36.51

C

C=====

C

C===== 6.0 Lower Chest Organ =====

C

C=====

C 6.1 U. bladder

C

C Mucosa wall

C=====

75 21 -1.04 -260 259 VOL = 5.3358402

C

C=====

C Remainder wall

C=====

76 21 -1.04 -258 260 VOL = 29.1641598

C=====

C Contents

C=====

77 21 -1.04 -259 VOL = 154

C

C=====

C

C===== 8.0 Gender Specific Organs =====

C

C=====

C

C=====

C 8.2 Female

C=====

C

C

C=====

C 8.2.1 Ovaries

C=====

C left

78 23 -1.05 -272 VOL=5.05

C right

79 23 -1.05 -273 VOL=5.05

C

C=====

C 8.2.2 Uterus

C=====

80 24 -1.02 -274 275 VOL=76

C

C=====

C 8.2.3 Breasts

C=====

C left gland

81 25 -0.94 -276 342 VOL=235.921

C right gland

82 25 -0.94 -277 342 VOL=235.921

C

C=====

C 9.0 Muscle in the Trunk

C=====

C

83 12 -1.03 341 -88 -342 -343 +344

C remove spine

(85:-86:88)

C remove trachea

(55:-57:53)

C remove (ribs 1-9)

(90:-91:92:-93) (90:-91:94:-95) (90:-91:96:-97)

(90:-91:98:-99) (90:-91:100:-101) (90:-91:102:-103)

(90:-91:104:-105) (90:-91:106:-107) (90:-91:108:-109)

(90:-91:110:-111) (90:-91:112:-113) (90:-91:114:-115)

C remove clavicles (left / right)

(116:-117:119) (116:118:-120)

C remove scapulae (left / right)

(-90:121:-122:124:-126:127)

(-90:121:123:-125:-126:127)

C remove pelvis

#31

C remove main bronchi

(144:146:-147:57:-154:-339)(148:150:-151:57:-155:339)

C remove lungs (left / right)

(154:92:-156:(-163 -162 -161))

(155:92:-156:(159 -160 -158 157))

C remove thymus

164

C remove heart

#38 #39

C remove adrenals (left / right)
 (177:-179) (178:-179)
 C remove kidneys (left / right)
 (181:183)(180:-182)
 C remove liver
 (204:205:206:-207)
 C remove gall bladder
 (212:209) (-212:211:213)
 C remove pancreas
 (214:-215:(-216 217))
 C remove spleen
 218
 C remove esophagus
 (221:88:-206)(223:-224:225)
 C remove stomach
 227
 C remove s. intestine
 (128:-230:231:-232:207)
 C remove a. colon
 (232:235:-237)
 C remove d. colon
 (232:245:-247)
 C remove s. colon
 (250:-247) (252:247)
 C remove rectum
 (256:247:-341)
 C remove u. bladder
 258
 C remove ovaries
 272 273
 C remove uterus
 (274:-275)

C
 VOL = 24297.269 \$Check this, removed prostate!!

C
 C=====

C 10.0 Skin
 C=====

C 10.2.2 Skin of Female Trunk (includes BREAST)
 C=====

C
 84 11 -1.09 ((-278 +342 -343 +344 -88 +341):
 (-278 +10 -345 +346 -283 +88):
 (-278 -345 +343 -88 +341):
 (-278 -344 +346 -88 +341):

C plus breast part
 (342 ((-279 276):(-280 277))))
 C remove material under neck
 (10:-88:283)
 C remove material under breast area (left / right)
 (-342:278:276) (-342:278:277)
 VOL = 958

C

C

C =====

C =====

C ARMS and LEGS for PIMAL

C =====

C ===== RIGHT ARM — BONE

85 2 -1.4 -289 +290 +294

86 2 -1.4 -290 +291

87 2 -1.4 -291

88 2 -1.4 -292 +291 +290

C ===== RIGHT ARM — SOFT TISSUE

89 13 -1.05 -293 +289 +290 +294

90 13 -1.05 -294 +290 +292

91 13 -1.05 -295 +290 +291 +292 +294 +296

92 13 -1.05 -296 +292 +294

C ===== RIGHT ARM — SKIN

c 93 11 -1.09 -297 +293 +294 +298

c 94 11 -1.09 -298 +294 +296

c 95 11 -1.09 -299 +294 +295 +296 +298 +300

c 96 11 -1.09 -300 +296 +298 +295

C

C ===== LEFT ARM — BONE

97 2 -1.4 -301 +302 +306

98 2 -1.4 -302 +303

99 2 -1.4 -303

100 2 -1.4 -304 +303 +302

C ===== LEFT ARM — SOFT TISSUE

101 13 -1.05 -305 +301 +302 +306

102 13 -1.05 -306 +302 +304

103 13 -1.05 -307 +302 +303 +304 +306 +308

104 13 -1.05 -308 +304 +306

C ===== LEFT ARM — SKIN

c 105 11 -1.09 -309 +305 +306 +310

c 106 11 -1.09 -310 +306 +308

c 107 11 -1.09 -311 +306 +307 +308 +310 +312

c 108 11 -1.09 -312 +308 +310 +307

C

C

c ===== RIGHT LEG — BONE

109 2 -1.4 -313 -341

110 2 -1.4 (-314 -341 315 313):(341 -314 315 313 278)

111 2 -1.4 -315

112 2 -1.4 -316 315 314

c ===== RIGHT LEG — TISSUE

113 13 -1.05 -317 -341 313 314 334

114 13 -1.05 (-318 314 315 316 317 -346):(346 -341 -318 315 314 316 317):(-318 314 315 316 317 341 278)

115 13 -1.05 -319 314 315 316 318 320

116 13 -1.05 -320 316 318

c ===== RIGHT LEG — SKIN

117 11 -1.09 -321 -341 322 317 334

118 11 -1.09 (-322 318 319 320 317 -346):(346 318 319 320 317 -322 -341):(-322 318 319 320 317 341 278)

119 11 -1.09 -323 318 319 320 322 324

120 11 -1.09 -324 319 320 322

c

c

c ===== LEFT LEG — BONE

121 2 -1.4 -325 -341

122 2 -1.4 (-326 -341 327 325):(-326 341 278 327 325)

123 2 -1.4 -327

124 2 -1.4 -328 327 326

c ===== LEFT LEG — TISSUE

125 13 -1.05 -329 -341 325 326 322

126 13 -1.05 (-330 326 327 328 329 345):(326 -330 327 328 329 -345 -341):(-330 326 327 328 329 341 278)

127 13 -1.05 -331 326 327 328 330 332

128 13 -1.05 -332 328 330

c ===== LEFT LEG — SKIN

129 11 -1.09 -333 -341 334 329 322

130 11 -1.09 (-334 330 331 332 329 345):(-334 330 331 332 329 -345 -341):(-334 330 331 332 329 341 278)

131 11 -1.09 -335 330 331 332 334 336

132 11 -1.09 -336 331 332 334

C

C

c =====

c Contamination

c =====

c ===== Head and Neck

c ——— top of the head ———

501 33 -0.0012 (-508 8 7)

c — face —
1501 33 -0.0012 ((-501 -4 32 33 -7 ((1 5):(-5 505 10))) #21 #20)
c — back of the head —
2501 33 -0.0012 ((-513 13 85 505 4 -7): (-501 1 -13 -7 4 505))
c — neck —
3501 33 -0.0012 (-505 -510 10 512 283)
c ===== Nose
521 33 -0.0012 ((-571 -572 73 501 -76 -75 71)
:(-571 -572 73 501 -76 74 72))
c ===== Trunk
c — Trunk —
584 33 -0.0012 (((-778 278 -345 346 -283 341):
(-778 -845 345 -283 341):
(-778 -346 846 -283 341))
c remove material under neck
(510:-283:783)
c remove material under breast area (left/right)
(-278:778:279) (-278:778:280) 780 779
c remove material inside arms
(298 310))
c — top of trunk —
684 33 -0.0012 (-778 510 -845 846 -783 283)
c — breasts —
784 33 -0.0012 (278 (-779 279))
884 33 -0.0012 (278 (-780 280))
c =====Arm
c — Right Arm —
593 33 -0.0012 (-797 297 298 798)
594 33 -0.0012 (-798 298 300 -846)
595 33 -0.0012 (-799 298 299 300 798 800)
596 33 -0.0012 (-800 300 798 299)
c — Left Arm —
605 33 -0.0012 (-809 309 310 810)
606 33 -0.0012 (-810 310 312 845)
607 33 -0.0012 (-811 310 311 312 810 812)
608 33 -0.0012 (-812 312 810 311)
c ===== Legs
c — Right Leg —
617 33 -0.0012 (-821 -341 822 321 834)
618 33 -0.0012 ((-822 322 323 324 321 -346)
:(346 322 323 324 321 -822 -341)
:(-822 322 323 324 321 341 778))
619 33 -0.0012 (-823 322 323 324 822 824)
620 33 -0.0012 (-824 323 324 822)
c — Left Leg —

629 33 -0.0012 (-833 -341 834 333 822)
 630 33 -0.0012 ((-834 334 335 336 333 345)
 :(-834 334 335 336 333 -345 -341)
 :(-834 334 335 336 333 341 778))
 631 33 -0.0012 (-835 334 335 336 834 836)
 632 33 -0.0012 (-836 335 336 834)
 c =====
 c Dermis/Epidermis
 c =====
 c ----- Arms -----
 1093 11 -1.09 -793 293 294 298
 1094 11 -1.09 -794 294 296
 1095 11 -1.09 -795 294 295 296 298 300
 1096 11 -1.09 -796 296 298 295
 2093 11 -1.09 -297 793 294 298
 2094 11 -1.09 -298 794 796
 2095 11 -1.09 -299 294 795 296 298 300
 2096 11 -1.09 -300 796 298 295
 1105 11 -1.09 -805 305 306 310
 1106 11 -1.09 -806 306 308
 1107 11 -1.09 -807 306 307 308 310 312
 1108 11 -1.09 -808 308 310 307 900
 2105 11 -1.09 -309 805 306 310
 2106 11 -1.09 -310 806 808
 2107 11 -1.09 -311 306 807 308 310 312
 2108 11 -1.09 -312 808 310 307
 C =====
 C GM Cells
 c =====
 801 31 -0.0008698 -401:-415 \$fill gas
 802 32 -7.8 -416 401 415:-417:-418 419 \$ steel casing
 803 33 -0.0012 -403:-406 420 421 422 423 424 425 426 427 428 429 430 431 432
 433 434 435 436 437 438 439:-407 402 415 416 417 418 419:-409 419
 \$air
 804 34 -2.6989 -405 402 403 406 407 420 421 422 423 424 425 426 427 428 429 430
 431 432 434 435 436 437 438 439 416:-408 407 409:-410 409 407:-420:-
 421
 :-422:-423:-424:-425:-426:-427:-428:-429:-430:-431:-432:-433
 :-434:-435:-436:-437:-438:-439 \$ aluminum mesh
 805 35 -0.94 -411:-412:-413:-414 \$ poly
 806 36 -8.96 -419 \$ copper wire
 c add cell 807 to cell 133 and change cell 133 to air
 c 807 33 -0.0012 -199 105 106 108 110 111 112 113 114 119 150 160:-151 153 160
 c :-152 151:-154 160 \$air
 810 40 -0.017 -402 401 403 415 416 \$ Mica window

```

c =====
c Tally Area
2900 11 -1.09 -900 -808 308
C =====
C Air Around the phantom
C =====
C
133 33 -0.0012 -338
C remove head and neck
      ((1:-12:(8 7)):(1:-12:(-5 10 12))
      :(1:-12:(4 -7 5 13)))
C remove nose
      (71:72:-73:-1:76)
C remove trunk region
      (-341:278:283:-346:345)
C remove breast region
      (-278:(279 280))
      +297 +298 +299 +300 +309 +310 +311 +312 $Exclude Arms
      +321 +322 +323 +324 +333 +334 +335 +336 $Exclude Legs
      405 406 408 410 411 412 413 414 419 $Excludes GM
c exclude head and neck contamination
      ((501:-12:(508 7)):(501:-12:(-505 510 512)):(501:-12:(4 -7 505 513)))
c exclude nose contamination
      (571:572:-73:-501:76)
c exclude trunk contamination
      (-341:778:783:-846:845)
c exclude breast contamination
      (-778:(779 780))
c exclude arm contamination (left/right)
      (797 798 799 800) (809 810 811 812)
c exclude leg contamination (left/right)
      (821 822 823 824) (833 834 835 836)
C
C =====
134 0 338 $OUTSIDE
C =====

C =====
C Surface Descriptions
C =====
C
C ===== OUTSIDE =====
C
338 so 200
C =====

```

```

C
C=====
C 1.0 Head and Neck Region
C=====
c
C 1.1 The skin of head
C
C Skin in the Face *
C=====
C
1 SQ 0.017313 0.011317 0 0 0 0 -1 0 0 0
2 SQ 0.018114 0.011738 0 0 0 0 -1 0 0 0
3 PY 4.53
4 PY 4.7
5 PZ 67.3
6 PZ 67.47
7 PZ 80.22
C=====
C Skin in the TOP OF the Head *
C=====
8 SQ 0.017313 0.011317 0.030036 0 0 0 -1 0 0 80.22
9 SQ 0.018114 0.011738 0.031888 0 0 0 -1 0 0 80.22
C=====
C Skin in the Neck*
C=====
10 SQ 1 1 0 0 0 0 -25.0000 0 1.78 0
11 SQ 1 1 0 0 0 0 -23.3289 0 1.78 0
12 PZ 63.1
C=====
C Skin in the BACK of the head*
C=====
13 K/Z 0 1.78 42.64351145 .4112231498e-1
14 K/Z 0 1.78 43.96522901 .4222622069e-1
C=====
C 1.2 The Cranium
C=====
C
C Cranium_Inner Surface
15 SQ 0.020525 0.012972 0.037704 0 0 0 -1 0 0 80.22
16 SQ 0.020525 0.012972 0.026612 0 0 0 -1 0 0 80.22
17 P 0 0.698178 1 74.09
18 PY 0
C=====
C Cranium_Outer Surface*
C=====

```

19 SQ 0.018114 0.011738 0.031888 0 0 0 -1 0 0 80.22
20 SQ 0.018114 0.011738 0.023097 0 0 0 -1 0 0 80.22
21 P 0 .7128927413 1 73.64

C=====

C 1.3 Teeth *

C=====

22 SQ 0.051187 0.037998 0 0 0 0 -1 0 -3.81 0
23 SQ 0.094095 0.046448 0 0 0 0 -1 0 -3.81 0
24 PZ 69.97
25 PZ 72.22
26 PY -3.81

C=====

C 1.4 Mandible *

C=====

27 SQ .02652548037 .3799839648e-1 0 0 0 0 -1 0 -3.81 0
28 SQ .09409462158 .7547397656e-1 0 0 0 0 -1 0 -3.81 0
29 PZ 68
30 SQ .06157294238 .1851080569e-1 0 0 0 0 -1 0 -3.81 0

C=====

C 1.5 Upper Face Regions *

C=====

31 SQ 0.022613 0.012237 0 0 0 0 -1 0 0 0

C=====

C 1.6 Eyes *

C=====

32 SQ 1 1 1 0 0 0 -1.2996 3.25 -7.06 76.72
33 SQ 1 1 1 0 0 0 -1.2996 -3.25 -7.06 76.72

C=====

C 1.7 Brain *

C=====

34 SQ 0.021004 0.013212 0.038903 0 0 0 -1 0 0 80.22
35 SQ 0.021004 0.013212 0.027321 0 0 0 -1 0 0 80.22
36 P 0 0.695402 1 74.17
37 PY 4.12

C=====

C 1.8 Spine in Head and Neck

C=====

38 SQ 0.212364 0.358564 0 0 0 0 -1 0 3.62 0

C=====

C

C

C 1.9 Sphenoid Sinus * *

C=====

39 SQ 2.137409801 1.085069445 3.293796794 0 0 0 -1 1.2 -4.8 76.12
40 SQ 2.137409801 1.085069445 3.293796794 0 0 0 -1 -1.2 -4.8 76.12

```

C=====
C 1.10 Ethmoid Sinus * *
C=====
41 SQ 8.070764463 1.108033241 1.462140076 0 0 0 -1 1.166 -6.7 76.52
42 SQ 8.070764463 1.108033241 1.462140076 0 0 0 -1 -1.166 -6.7 76.52
C=====
C 1.11 Frontal Sinus * *
C=====
C
43 SQ 1.108033241 3.293796794 .5266251124 0 0 0 -1 1.5 -8.1 77.9
44 SQ 1.108033241 3.293796794 .5266251124 0 0 0 -1 -1.5 -8.1 77.9
C
C=====
C 1.12 Maxillary Sinus*
C=====
45 S 2.9 -6.2 74.02 1.374
46 S -2.9 -6.2 74.02 1.374
C=====
C 1.13 Pharynx *
C=====
47 C/Z 0 1.96 1.08
48 C/Z 0 1.96 0.84
49 PZ 73.55
C
50 C/Z 0 1.96 0.933
C=====
C 1.14 Larynx*
C=====
51 C/Z 0 -0.13 0.59
52 C/Z 0 -0.13 0.83
53 PZ 63.67
C
54 C/Z 0 -0.13 0.683
C=====
C 1.15 Trachea *
C=====
55 C/Z 0 -0.13 1.0
56 C/Z 0 -0.13 0.74
57 PZ 56.23
C
58 C/Z 0 -0.13 0.793
C=====
C 1.16 Thyroid **
C=====
59 C/Z 0 -0.13 1.647

```

60 C/Z 0 -0.13 0.83
 61 P .5868986284 -.7168986284 67.3 0 -0.96 64.15 0 -1.98 65.65
 62 P -.5868986284 -.7168986284 67.3 0 -0.96 64.15 0 -1.98 65.65
 63 P .5868986284 -.7168986284 63.1 0 -0.96 64.15 0 -1.98 63.625
 64 P -.5868986284 -.7168986284 63.1 0 -0.96 64.15 0 -1.98 63.625
 65 PY -0.13
 66 PZ 64.15
 67 PZ 63.1
 C
 C =====
 C 1.17 Nose*
 C =====
 68 P 0 -9.4 77.02 -1.416 -9.235405171 71.97 0 -10.654 74.495
 69 P 0 -9.4 77.02 1.416 -9.235405171 71.97 0 -10.654 74.495
 70 P 0 -11.528 71.97 -1.416 -9.235405171 71.97 1.416 -9.235405171 71.97
 C
 71 P 0 -9.78 77.02 -1.796 -9.133757296 71.97 0 -11.034 74.495
 72 P 0 -9.78 77.02 1.796 -9.133757296 71.97 0 -11.034 74.495
 73 P 0 -11.528 71.59 -1.416 -9.235405171 71.59 1.416 -9.235405171 71.59
 C
 74 PX -0.19
 75 PX 0.19
 C
 76 PY -8.4
 C =====
 C 1.19 Salivary Glands
 C
 C =====
 C 1.19.1 Parotids Glands
 C =====
 C Left
 C
 77 SQ 1.200449511 0.2770083103 0 0 0 0 -1 1.875 -1.905 71.735
 C
 C Right
 C
 78 SQ 1.200449511 0.2770083103 0 0 0 0 -1 -1.875 -1.905 71.735
 C =====
 C 1.19.2 Submandibular Glands
 C =====
 C Left
 C
 79 C/Z 1.75 -2.305 1.495
 80 PZ 69.369
 C

C Right
 C
 81 C/Z -1.75 -2.305 1.495
 C =====
 C 1.19.3 Sublingual Glands
 C =====
 C Left
 C
 82 C/Y 0.7 69.369 0.601
 83 PY -7.2
 C
 C Right
 C
 84 C/Y -0.7 69.369 0.601
 C
 C =====
 C
 C ===== 2.0 Skeleton* =====
 C
 C =====
 C 2.1 Spine (1983 /C&E)*
 C
 85 SQ .1665972511 .3341240937 0 0 0 0 -1 0 4.775 0
 86 PZ 19.83
 87 PZ 31.64
 88 PZ 63.1
 89 PZ 72.91
 C
 C =====
 C 2.2 Ribs (outer surface / inner surface)*
 C =====
 90 SQ 92.26 214.92 0 0 0 0 -19806.62 0 0 0
 91 SQ 83.36 201.36 0 0 0 0 -16784.42 0 0 0
 C
 92 PZ 60.65
 93 PZ 59.39
 94 PZ 58.13
 95 PZ 56.87
 96 PZ 55.61
 97 PZ 54.35
 98 PZ 53.09
 99 PZ 51.83
 100 PZ 50.57
 101 PZ 49.31
 102 PZ 48.05

103 PZ 46.79
104 PZ 45.53
105 PZ 44.27
106 PZ 43.01
107 PZ 41.75
108 PZ 40.49
109 PZ 39.23
110 PZ 37.97
111 PZ 36.71
112 PZ 35.45
113 PZ 34.19
114 PZ 32.93
115 PZ 31.67

C=====

C 2.3 Clavicles*

C=====

116 TZ 0 7.22 61.52 15.93 0.7274 0.7274
117 P 6.4852 1 0 7.22
118 P 6.4852 -1 0 -7.22
119 P 0.73137 1 0 7.22
120 P 0.73137 -1 0 -7.22

C

C=====

C 2.4 Scapulae (inner surface / outer surface)*

C=====

121 SQ 92.16 267.65 0 0 0 0 -24666.59 0 0 0
122 P 0.28 1 0 0
123 P 0.28 -1 0 0
124 P 0.91 1 0 0
125 P 0.91 -1 0 0
126 PZ 45.88
127 PZ 60.67

C=====

C 2.5 Pelvis*

C=====

128 SQ 122.54 95.06 0 0 0 0 -11649.4246 0 -3.72 0
129 SQ 138.30 107.12 0 0 0 0 -14814.78 0 -2.94 0
130 PY -2.94
131 PY 4.9
132 PZ 19.83
133 PZ 12.62

C

C=====

C 3.0 Upper Chest Organs

C

```

C=====
C 3.1 Main Bronchi*
C=====
144 7 CZ 0.741
145 7 CZ 0.504
146 7 PZ 4.92
147 7 PZ -4.92
C
148 8 CZ 0.741
149 8 CZ 0.504
150 8 PZ 4.92
151 8 PZ -4.92
C
152 7 CZ 0.558
153 8 CZ 0.558
C=====
C 3.2 Lungs*
C (left / right)
C=====
154 SQ .5977965220e-1 .2052528303e-1 .2367970827e-2 0 0 0 -1 7.33 0 39.21
155 SQ .5977965220e-1 .2052528303e-1 .2367970827e-2 0 0 0 -1 -7.33 0 39.21
156 PZ 39.21
157 PX -5.0
158 PY 1.2
159 PZ 41.6
160 PZ 48.5
161 PX 7
162 PY 0.7
163 PZ 49
C=====
C 3.3 Thymus*
C=====
164 SQ .2921840759 .9425959091 .5948839975e-1 0 0 0 -1 0 -7.15 52
C
C=====
C 3.4 Heart Model *
C=====
C basic planes
165 4 PX 0
166 4 PZ 0
C
C right ventricle
167 4 SQ .1618657291e-1 .4788148373e-1 .2441406250e-1 0 0 0 -1 0 0 0
168 4 SQ .01871394057 .6187965644e-1 .2922054203e-1 0 0 0 -1 0 0 0
C

```

C left ventricle

169 4 SQ .1618657291e-1 .4788148373e-1 .1248610921 0 0 0 -1 0 0 0

170 4 SQ .2247751687e-1 .8753194918e-1 .3718024986 0 0 0 -1 0 0 0

C

C left atrium, part 1

171 4 SQ .4097756069e-1 .4788148373e-1 .1248610921 0 0 0 -1 0 0 0

172 4 SQ .04585283989 .5408328825e-1 .1525878906 0 0 0 -1 0 0 0

C

C left atrium, part 2

173 4 SQ .04097756069 .4788148373e-1 .2741152929 0 0 0 -1 0 0 0

174 4 SQ .04585283989 .5408328825e-1 .3718024986 0 0 0 -1 0 0 0

C

C right atrium

175 4 SQ .4097756069e-1 .4788148373e-1 .2441406250e-1 0 0 0 -1 0 0 0

176 4 SQ .04585283989 .5408328825e-1 .2661209412e-1 0 0 0 -1 0 0 0

C

C =====

C

C ===== 4.0 Middle Chest Organs =====

C

C =====

C

C 4.1 Adrenals (left / right)*

C =====

177 1 SQ .5917159763 5.408328825 .5408328825e-1 0 0 0 -1 0 0 0

178 2 SQ .5917159763 5.408328825 .5408328825e-1 0 0 0 -1 0 0 0

179 PZ 34.26

C

C =====

C 4.2 Kidneys (left / right)*

C =====

C

180 SQ .06096631609 .4271861249 .4064776274e-1 0 0 0 -1 5.18 5.88 29.3

181 SQ .06096631609 .4271861249 .4064776274e-1 0 0 0 -1 -5.18 5.88 29.3

182 PX 2.48

183 PX -2.48

C

202 PX 2.48

203 PX -2.48

C

C =====

C 4.3 Liver *

C =====

204 SQ 61.47 201.36 0 0 0 0 -12376.4735 0 0 0

205 P .3173595684e-1 .2234636872e-1 -.2579979360e-1 -1

206 PZ 38.76
 207 PZ 24.34
 C
 C=====

C 4.4 Gall bladder*
 C=====

208 3 SO 1.916
 209 3 SO 2.015
 210 3 GQ 1 1 -.5175625000e-1 0 0 0 0 0 .8717800000 -3.671056000
 211 3 GQ 1 1 -.5175625000e-1 0 0 0 0 0 .9168250000 -4.060225000
 212 3 PZ 0
 213 3 PZ 7.66
 C
 C=====

C 4.5 Pancreas *
 C=====

C
 214 SQ .4271861249e-2 .7694675285 .5948839975e-1 0 0 0 -1 -1.22 0 31.85
 215 PX -1.22
 216 PZ 31.85
 217 PX 2.11
 C
 C=====

C 4.6 Spleen *
 C=====

218 SQ 95.20 226.53 29.72 0 0 0 -800.6568 9.49 2.94 33.35
 C
 C=====

C
 C===== 5.0 Gastrointestinal tract and contents =====

C
 C=====

C 5.1 Male Esophagus*
 C=====

219 6 CX 0.070
 220 SQ 1.417233560 27.70083102 0 0 0 0 -1 0 2.29 0
 221 SQ 0.16 1.1025 0 0 0 0 -0.1764 0 2.29 0
 222 SQ 0.0144 0.5929 0 0 0 0 -0.00854 0 2.29 0
 C
 C 409 0.64 cm -ç 0.5504 cm
 223 6 CX 0.5504
 224 6 PX 0.0
 225 6 PX 7.07
 C
 C=====

C 5.2 Stomach *

C=====

C

226 SQ .1052090140 .1510498950 .2154384531e-1 0 0 0 -1 6.9 -3.92 31.55

227 SQ 437.11 603.135 100.312 0 0 0 -5142.57 6.9 -3.92 31.55

228 SQ 242.612 358.799 45.876 0 0 0 -1998.369 6.9 -3.92 31.55

C

C=====

C 5.3 S. intestine *

C=====

C

229 SQ 122.54 95.06 0 0 0 0 -11649.4246 0 -3.72 0

230 PY -4.76

231 PY 2.16

232 PZ 15.32

233 PZ 24.34

C

C=====

C 5.4 A. colon*

C=====

234 SQ .3505425171 .2553338605 0 0 0 0 -1 -7.33 -2.31 0

235 SQ .2143545522 .1666108517 0 0 0 0 -1 -7.33 -2.31 0

236 SQ 3.24 2.2801 0 0 0 0 -7.3875 -7.33 -2.31 0

237 PZ 13.03

238 PZ 21.63

C

C=====

C 5.5 T. colon*

C=====

239 SQ 0 .2278410353 1.010075503 0 0 0 -1 0 -2.31 22.99

240 SQ 0 .1666108517 .5487781425 0 0 0 -1 0 -2.31 22.99

241 SQ 0 0.7396 3.8416 0 0 0 -2.8412 0 -2.31 22.99

242 PX 9.06

243 PX -9.06

C

C=====

C 5.6 D. colon*

C=====

244 GQ .7790048836 .4200182372 .1515605581e-1 0 .1494618274 -.7612410830e-1

-10.78635348 -1.174769963 .3180008868 37.15927759

245 GQ .4385772553 .2712673611 .9634411191e-2 0 .9652941682e-1 -.4285762924e-

1

-6.072682475 -.7587212163 .1617163245 20.55160754

246 GQ 1.020304050 .5102040817 .1858708278e-1 0 .1815541031 -.9970378577e-1

-14.12745976 -1.427015251 .4363665620 48.90116638

247 PZ 7.86
C
C=====

C 5.7 S. colon
C=====

248 TY 1.18 0 7.86 1.18 1.463 0.883
249 TY 4.8336 0 7.86 2.4736 1.463 0.883
C
250 TY 1.18 0 7.86 1.18 1.76 1.18
251 TY 1.18 0 7.86 1.18 1.35 0.77
252 TY 4.8336 0 7.86 2.4736 1.76 1.18
253 TY 4.8336 0 7.86 2.4736 1.35 0.77
254 PX 3
C
C=====

C 5.8 Rectum
C=====

255 SQ .9592869045 .3901371761 0 0 0 0 -1 0 0 0
256 SQ 3.0976 1.3924 0 0 0 0 -4.3131 0 0 0
257 SQ 2.3716 0.9216 0 0 0 0 -2.1857 0 0 0
C
C=====

C
C===== 6.0 Lower Chest Organs =====

C
C=====

C 6.1 U. bladder
C=====

258 SQ 110.4979 176.3504 208.2999 0 0 0 -2014.6979 0 -5.15 7.21
259 SQ 82.3012 135.3779 161.9511 0 0 0 -1343.2970 0 -5.15 7.21
260 SQ .06004361208 .9820789256e-1 .1172025028 0 0 0 -1 0 -5.15 7.21
C
C=====

C
C=====

C 8.2 Female
C=====

C 8.2.1 Ovaries (left / right)*
C=====

C Ovaries (left / right)(Shifted -0.1cm x-direction w/ lower abs)
C=====

272 SQ .7305135510 2.972651605 .3086419754 0 0 0 -1 5.08 0 13.52
273 SQ .7305135510 2.972651605 .3086419754 0 0 0 -1 -5.08 0 13.52
C
C=====

C 8.2.2 Uterus *
C=====

274 SQ 75.6117 14.6574 192.0071 0 0 0 -461.2995 0 -1.96 12.62

275 PY -4.77

C

C=====

C 8.2.3 Breasts *

C=====

C left

276 SQ .3648939207e-1 .4654794612e-1 .5084084402e-1 0 0 0 -1.0

8.63 -8.485408314 46.87

C

C right

277 SQ .3648939207e-1 .4654794612e-1 .5084084402e-1 0 0 0 -1.0

-8.63 -8.485408314 46.87

C

C=====

C

C===== 10.0 Skin surface descriptions =====

C

C=====

C

C 10.2 Trunk*

C=====

278 SQ 99.4 303.4564 0 0 0 0 -30163.8393 0 0 0

C

C 10.2.2 Female Trunk

C

279 SQ .3423013431e-1 .4331249643e-1 .4715640955e-1 0 0 0 -1 8.63

-8.485408314 46.87

C

280 SQ .3423013431e-1 .4331249643e-1 .4715640955e-1 0 0 0 -1 -8.63

-8.485408314 46.87

C plane above torso

283 PZ 63.27

C

C=====

C===== START CHANGES FOR ARMS AND LEGS HERE =====

C=====

C

C===== RIGHT ARM — BONE

289 sph -20.25 0 58.6 2.75

290 trc -20.25 0 58.6 0 0 -31 2.80 2.05

291 sph -20.25 0 27.6 1.95

292 trc -20.25 0 27.6 0 0 -27.3 2.05 1.5

C===== RIGHT ARM — SOFT TISSUE

293 sph -20.25 0 58.6 4.5

294 trc -20.25 0 58.6 0 0 -31 4.55 4.0
 295 sph -20.25 0 27.6 4.0
 296 trc -20.25 0 27.6 0 0 -27.3 4.0 3.0
 C ===== RIGHT ARM — SKIN
 297 sph -20.25 0 58.6 4.7
 298 trc -20.25 0 58.6 0 0 -31 4.75 4.2
 299 sph -20.25 0 27.6 4.2
 300 trc -20.25 0 27.6 0 0 -27.3 4.2 3.2
 C ===== LEFT ARM — BONE
 301 sph 20.25 0 58.6 2.75
 302 trc 20.25 0 58.6 0 0 -31 2.80 2.05
 303 sph 20.25 0 27.6 1.95
 304 trc 20.25 0 27.6 0 0 -27.3 2.05 1.5
 C ===== LEFT ARM — SOFT TISSUE
 305 sph 20.25 0 58.6 4.5
 306 trc 20.25 0 58.6 0 0 -31 4.55 4.0
 307 sph 20.25 0 27.6 4.0
 308 trc 20.25 0 27.6 0 0 -27.3 4.0 3.0
 C ===== LEFT ARM — SKIN
 309 sph 20.25 0 58.6 4.7
 310 trc 20.25 0 58.6 0 0 -31 4.75 4.2
 311 sph 20.25 0 27.6 4.2
 312 trc 20.25 0 27.6 0 0 -27.3 4.2 3.2
 C
 C
 C ===== RIGHT LEG — BONE
 313 sph -7.7 0.0 -3.01 4.75
 314 trc -7.7 0.0 -3.1 0.00 0.00 -36.50 4.5 2.75
 315 sph -7.7 0.0 -39.51 2.75
 316 trc -7.7 0.0 -39.51 0.00 0.00 -38.70 2.85 1.85
 C ===== RIGHT LEG – SOFT TISSUE
 317 sph -7.7 0 -3.01 7.45
 318 trc -7.7 0 -3.1 0.00 0.00 -36.50 7.05 6.05
 319 sph -7.7 0.00 -39.51 6.05
 320 trc -7.7 0.00 -39.51 0.00 0.00 -38.70 6.05 5.05
 C ===== RIGHT LEG – SKIN
 321 sph -7.7 0 -3.01 7.65
 322 trc -7.7 0 -3.1 0.00 0.00 -36.50 7.25 6.25
 323 sph -7.7 0.00 -39.51 6.25
 324 trc -7.7 0.00 -39.51 0.00 0.00 -38.70 6.25 5.25
 C ===== LEFT LEG – BONE
 325 sph +7.7 0 -3.01 4.75
 326 trc +7.7 0 -3.1 0.00 0.00 -36.50 4.5 2.75
 327 sph +7.7 0.0 -39.51 2.75
 328 trc +7.7 0.0 -39.51 0.00 0.00 -38.70 2.85 1.85

```

C ===== LEFT LEG – SOFT TISSUE
329 sph +7.7 0 -3.01 7.45
330 trc +7.7 0 -3.1 0.00 0.00 -36.50 7.05 6.05
331 sph +7.7 0.0 -39.51 6.05
332 trc +7.7 0.0 -39.51 0.00 0.00 -38.70 6.05 5.05
C ===== LEFT LEG – SKIN
333 sph +7.7 0 -3.01 7.65
334 trc +7.7 0 -3.1 0.00 0.00 -36.50 7.25 6.25
335 sph +7.7 0.0 -39.51 6.25
336 trc +7.7 0.0 -39.51 0.00 0.00 -38.70 6.25 5.25
C ===== STOP CHANGES FOR ARMS AND LEGS HERE =====
C
C =====
339 PX 0
340 PY 0
341 PZ 0
C outer ellipsoid
342 SQ .3360638521e-2 .1041232819e-1 0 0 0 0 -1 0 0 0
343 px +15.2
344 px -15.2
345 px +15.5
346 px -15.5
C =====
C
C =====
C Source Surfaces
c =====
c ===== Head and Neck
c ——— Face ———
501 SQ 0.01731074159 0.01131579724 0 0 0 0 -1 0 0 0
c 502 SQ 0.01811155505 0.01173671946 0 0 0 0 -1 0 0 0
c 503 PY 4.5305
c 504 PY 4.7005
505 PZ 67.2995
c 506 PZ 67.4705
c ——— Top of the Head ———
508 SQ 0.01731074159 0.01131579724 0.03003081291 0 0 0 -1
      0 0 80.22
c ——— Neck ———
510 SQ 0.99980003 0.99980003 0 0 0 0 -25.0 0 1.78 0
512 PZ 63.1005
c ——— Back of the Head ———
513 K/Z 0 1.78 42.64099562 0.4112231498E-1
c ===== Nose
571 P -2.69953481E-4 -9.780153709 77.02007634

```

-1.796269953 -9.133911005 71.97007634
 -2.69953481E-4 -11.03415371 74.49507634
 572 P 2.77147438E-4 -9.780142526 77.02008033
 1.796277147 -9.133899822 71.97008033
 2.77147438E-4 -11.03414253 74.49508033
 573 PZ 71.5895
 c ===== Trunk
 778 SQ 99.394053 303.4259656 0 0 0 0 -30163.8393 0 0 0
 779 SQ 0.03422380216 0.04330348377 0.04714617096 0 0 0 -1
 8.63 -8.485408314 46.86
 780 SQ 0.03422380216 0.04330348377 0.04714617096 0 0 0 -1
 -8.63 -8.485408314 46.86
 783 PZ 63.2705
 845 PX 15.5005
 846 PX -15.5005
 c ===== Arm
 c -----Right Arm -----
 797 SPH -20.25 0 58.6 4.7005
 798 TRC -20.25 0 58.6 0 0 -31 4.7505 4.2005
 799 SPH -20.25 0 27.6 4.2005
 800 TRC -20.25 0 27.6 0 0 -27.3 4.2005 3.2005
 c ----- Left Arm -----
 809 SPH 20.25 0 58.6 4.7005
 810 TRC 20.25 0 58.6 0 0 -31 4.7505 4.2005
 811 SPH 20.25 0 27.6 4.2005
 812 TRC 20.25 0 27.6 0 0 -27.3 4.2005 3.2005
 c ===== Legs
 c ----- Right Leg -----
 821 SPH -7.7 0 -3.01 7.6505
 822 TRC -7.7 0 -3.1 0 0 -36.50 7.2505 6.2505
 823 SPH -7.7 0 -39.51 6.2505
 824 TRC -7.7 0 -39.51 0 0 -38.70 6.2505 5.2505
 c ----- Left Leg -----
 833 SPH 7.7 0 -3.01 7.6505
 834 TRC 7.7 0 -3.1 0 0 -36.50 7.2505 6.2505
 835 SPH 7.7 0 -39.51 6.2505
 836 TRC 7.7 0 -39.51 0 0 -38.70 6.2505 5.2505
 c =====
 c Dermal/Epidermal Divide
 c =====
 c ----- Arms -----
 793 sph -20.25 0 58.6 4.693
 794 trc -20.25 0 58.6 0 0 -31 4.743 4.193
 795 sph -20.25 0 27.6 4.193
 796 trc -20.25 0 27.6 0 0 -27.3 4.193 3.193

805 sph 20.25 0 58.6 4.693
 806 trc 20.25 0 58.6 0 0 -31 4.743 4.193
 807 sph 20.25 0 27.6 4.193
 808 trc 20.25 0 27.6 0 0 -27.3 4.193 3.193

C =====

C GM

c =====

c ——— gas in detector ———

401 10 RCC 0.6 0 0 1.19 0 0 2.5297

c — inner detector casing —

402 10 RCC 0.4175 0 0 1.5494 0 0 2.6797

c – air cutout in the inner casing –

403 10 RCC 0.4175 0 0 0.05 0 0 2.2225

c — outer detector head —

405 10 RCC 0 0 0 2.54 0 0 3.4925

c — air cutout in outer casing —

406 10 RCC 0 0 0 0.4175 0 0 2.54

c — detector arm extension —

407 10 RCC 1.1922 -2.66 0 0 -3.40995 0 0.8025

408 10 RCC 1.1922 -2.91465 0 0 -3.175 0 0.9525

409 10 RCC 1.12 -5.6 0 5.3427 -14.6789 0 0.8025

410 10 RCC 1.12 -5.6 0 5.3427 -14.6789 0 0.9525

c — nubs on detector head —

411 10 RCC 0 3.016 0 -0.17 0 0 0.2

412 10 RCC 0 -3.016 0 -0.17 0 0 0.2

413 10 RCC 0 0 3.016 -0.17 0 0 0.2

414 10 RCC 0 0 -3.016 -0.17 0 0 0.2

c — extension of inner detector —

415 10 RCC 1.1922 -2.5296 0 0 -0.9629 0 0.485

416 10 RCC 1.1922 -2.5296 0 0 -0.9629 0 0.635

417 10 RCC 1.1922 -3.4925 0 0 -0.8128 0 0.35

418 10 RCC 1.1922 -4.3053 0 0 -0.635 0 0.3175

c — wire inside the handle —

419 10 RCC 1 -4.9403 0 5.5 -15.3386 0 0.01

c — wire mesh —

420 10 RCC 0.3 -2.52 0.25 0 5.04 0 0.03

421 10 RCC 0.3 -2.45 0.75 0 4.9 0 0.03

422 10 RCC 0.3 -2.2 1.25 0 4.4 0 0.03

423 10 RCC 0.3 -1.85 1.75 0 3.7 0 0.03

424 10 RCC 0.3 -1.15 2.25 0 2.3 0 0.03

425 10 RCC 0.3 -2.52 -0.25 0 5.04 0 0.03

426 10 RCC 0.3 -2.44 -0.75 0 4.88 0 0.03

427 10 RCC 0.3 -2.2 -1.25 0 4.4 0 0.03

428 10 RCC 0.3 -1.85 -1.75 0 3.7 0 0.03

429 10 RCC 0.3 -1.15 -2.25 0 2.3 0 0.03

430 10 RCC 0.3 0.25 -2.52 0 0 5.04 0.03
 431 10 RCC 0.3 0.75 -2.45 0 0 4.9 0.03
 432 10 RCC 0.3 1.25 -2.2 0 0 4.4 0.03
 433 10 RCC 0.3 1.75 -1.85 0 0 3.7 0.03
 434 10 RCC 0.3 2.25 -1.15 0 0 2.3 0.03
 435 10 RCC 0.3 -0.25 -2.52 0 0 5.04 0.03
 436 10 RCC 0.3 -0.75 -2.45 0 0 4.9 0.03
 437 10 RCC 0.3 -1.25 -2.2 0 0 4.4 0.03
 438 10 RCC 0.3 -1.75 -1.85 0 0 3.7 0.03
 439 10 RCC 0.3 -2.25 -1.15 0 0 2.3 0.03

c =====

c Tally Area

900 RCC 23.2 0 13.65 1 0 0 1.784124116

C =====

C =====

C ===== Axis Transformation Section * =====

C =====

C Adrenals (left / right)

C =====

TR1 3.22 4.9 34.26 0.5650 0.8251 0 -0.8251 0.5650 0 0 0 1

TR2 -3.22 4.9 34.26 0.5650 -0.8251 0 0.8251 0.5650 0 0 0 1

C =====

C Gall Bladder

C =====

TR3 -3.98 -3.14 27.04

0.9550 0 -0.2964 -0.0606 0.9789 -0.1952 0.2903 0.2044 0.9349

C =====

C Heart

C =====

TR4 0.86 -2.1 45.10

0.6453 -0.5134 -0.5658 -0.4428 0.3523 -0.8245

0.6226 0.7825 0

C =====

C Esophagus

C =====

TR6 0 2.29 38.08

0.708385 -0.637547 -0.302860 0.668965 0.743294 0 0.225114

-0.202603 0.953035

C =====

C Main Bronchi

C

C =====

*TR7 1.6 -0.13 54 33 90 57 90 0 90 123 90 33

*TR8 -1.6 -0.13 54 33 90 123 90 0 90 57 90 33

```

C =====
C GM Meter
C
C =====
TR10 24.95 0 13.65 1 0 0 0 1 0 0 0 1 1
C =====
C
C ===== MATERIAL CARDS =====
C
C =====
C ===== SKELETON – Density = 1.4 g/cc =====
C =====
M2 1001 -0.07337
      6000 -0.25475
      7014 -0.03057
      8016 -0.47893
      9019 -0.00025
      11023 -0.00326
      12000 -0.00112
      14000 -0.00002
      15031 -0.05095
      16000 -0.00173
      17000 -0.00143
      19000 -0.00153
      20000 -0.10190
      26000 -0.00008
      30000 -0.00005
C
C =====
C ===== AIR – Density = 0.001205 g/cc =====
C =====
M4 6000 -0.000124
      7014 -0.755267
      8016 -0.231781
      18000 -0.012827
C
C =====
C ===== UPPER FACE REGION – Density = 1.22 g/cc =====
C =====
M5 1001 -0.088955
      6000 -0.240690
      7014 -0.027735
      8016 -0.557090
      9019 -0.000125
      11023 -0.002190

```

12000 -0.000625
 14000 -0.000160
 15031 -0.026145
 16000 -0.001885
 17000 -0.001380
 19000 -0.001805
 20000 -0.051070
 26000 -0.000065
 30000 -0.000040
 40000 -0.000010
 82000 -0.000005

C

C=====

C===== BRAIN – Density = 1.04 g/cc =====

C=====

M6 1001 -0.107

6000 -0.145
 7014 -0.022
 8016 -0.712
 11023 -0.002
 15031 -0.004
 16000 -0.002
 17000 -0.003
 19000 -0.003

C

C=====

C===== EYES – Density = 1.07 g/cc =====

C=====

M7 1001 -0.096

6000 -0.195
 7014 -0.057
 8016 -0.646
 11023 -0.001
 15031 -0.001
 16000 -0.003
 17000 -0.001

C

C=====

C===== LARYNX – Density = 1.10 g/cc =====

C=====

C

M8 1001 -0.096

6000 -0.099
 7014 -0.022
 8016 -0.744

11023 -0.005
15031 -0.022
16000 -0.009
17000 -0.003

C

C=====

C===== TRACHEA – Density = 1.03 g/cc =====

C=====

C

M9 1001 -0.105

6000 -0.256
7014 -0.027
8016 -0.602
11023 -0.001
15031 -0.002
16000 -0.003
17000 -0.002
19000 -0.002

C

C=====

C===== THYROID – Density = 1.05 =====

C=====

M10 1001 -0.104

6000 -0.119
7014 -0.024
8016 -0.745
11023 -0.002
15031 -0.001
16000 -0.001
17000 -0.002
19000 -0.001

C

C=====

C===== SKIN – Density = 1.09 g/cc =====

C=====

C

M11 1001 -0.1

6000 -0.204
7014 -0.042
8016 -0.645
11023 -0.002
15031 -0.001
16000 -0.002
17000 -0.003
19000 -0.001


```

C
C=====
C===== SOFT TISSUE – Density = 1.03 g/cc =====
C=====
C
M12 1001 -0.105
      6000 -0.256
      7014 -0.027
      8016 -0.602
      11023 -0.001
      15031 -0.002
      16000 -0.003
      17000 -0.002
      19000 -0.002

C
C=====
C===== MUSCLE – Density = 1.05 g/cc =====
C=====
C
M13 1001 -0.102
      6000 -0.143
      7014 -0.034
      8016 -0.71
      11023 -0.001
      15031 -0.002
      16000 -0.003
      17000 -0.001
      19000 -0.004

C
C=====
C===== LUNGS – Density = 0.26 g/cc =====
C=====
C
M14 1001 -0.103
      6000 -0.105
      7014 -0.031
      8016 -0.749
      11023 -0.002
      15031 -0.002
      16000 -0.003
      17000 -0.003
      19000 -0.002

C
C=====
C===== HEART – Density = 1.05 g/cc =====

```

```

C =====
C
M15 1001 -0.104
      6000 -0.139
      7014 -0.029
      8016 -0.718
      11023 -0.001
      15031 -0.002
      16000 -0.002
      17000 -0.002
      19000 -0.003

C
C =====
C ===== KIDNEY – Density = 1.05 g/cc =====
C =====
M16 1001 -0.103
      6000 -0.132
      7014 -0.03
      8016 -0.724
      11023 -0.002
      15031 -0.002
      16000 -0.002
      17000 -0.002
      19000 -0.002
      20000 -0.001

C
C =====
C ===== LIVER – Density = 1.05 g/cc =====
C =====
C
M17 1001 -0.103
      6000 -0.186
      7014 -0.028
      8016 -0.671
      11023 -0.002
      15031 -0.002
      16000 -0.003
      17000 -0.002
      19000 -0.003

C
C =====
C ===== PANCREAS – Density = 1.04 g/cc =====
C =====
C
M18 1001 -0.106

```

6000 -0.169
7014 -0.022
8016 -0.694
11023 -0.002
15031 -0.002
16000 -0.001
17000 -0.002
19000 -0.002

C

C=====

C===== SPLEEN – Density = 1.06 g/cc =====

C=====

M19 1001 -0.103

6000 -0.113
7014 -0.032
8016 -0.741
11023 -0.001
15031 -0.003
16000 -0.002
17000 -0.002
19000 -0.003

C

C=====

C===== GI TRACT – Density 1.03 g/c =====

C=====

M20 1001 -0.106

6000 -0.115
7014 -0.022
8016 -0.751
11023 -0.001
15031 -0.001
16000 -0.001
17000 -0.002
19000 -0.001

C

C=====

C===== URINARY BLADDER – Density = 1.04 g/cc =====

C=====

C

M21 1001 -0.105

6000 -0.096
7014 -0.026
8016 -0.761
11023 -0.002
15031 -0.002

16000 -0.002
17000 -0.003
19000 -0.003

C

C=====

C===== TESTES – Density = 1.04 g/cc =====

C=====

C

M22 1001 -0.106

6000 -0.099
7014 -0.02
8016 -0.766
11023 -0.002
15031 -0.001
16000 -0.002
17000 -0.002
19000 -0.002

C

C=====

C===== OVARY – Density = 1.05 g/cc =====

C=====

C

M23 1001 -0.105

6000 -0.093
7014 -0.024
8016 -0.768
11023 -0.002
15031 -0.002
16000 -0.002
17000 -0.002
19000 -0.002

C

C=====

C===== UTERUS – Density = 1.02 g/cc =====

C=====

C

M24 1001 -0.106

6000 -0.315
7014 -0.024
8016 -0.547
11023 -0.001
15031 -0.002
16000 -0.002
17000 -0.001
19000 -0.002

```

C
C =====
C ===== BREAST – Density = 0.94 g/cc =====
C Composition information from ICRP-89, Table 13.3 on page 244
C Note: Female Breast Values are taken from this Table
C =====
C
M25 1001 -0.116
      6000 -0.519
      8016 -0.365

C =====
C GM Detector Materials
M31 10000 0.92 18000 0.075 35000 0.005 $ fill gas
M32 26000 0.75 24000 0.25 $ 446 SS
M33 7000 0.78 8000 0.21 18000 0.01 $Air
M34 13000 1 $ Aluminum
M35 6000 0.856 1000 0.144 $Polyethylene
M36 29000 1 $ Copper
M40 19000 0.043 13000 0.087 14000 0.174 8000 0.522 1000 0.087 9000 0.087
$ Mica
C =====
C TALLY DEFINITION SECTION
C =====
C
C ENDORGAN
C =====
c fc216 PHOTON contribution
c F216:p,e
C Organ: ovaries
c      (78 79)
C Organ: bone marrow
c      (2 3 4 5 $ Cranium and mandible
c      30 29 $ Scapulae and clavicle
c      28 $ ribs
c      31 ) $ pelvis
C Organ: colon
c      (57 58 $ right (mucosa+wall)
c      60 61 $ T colon (mucosa+wall)
c      63 64 $ left (mucosa+wall)
c      66 67 $ D colon (mucosa+wall)
c      69 70 $ sigmoid (mucosa+wall)
c      72 73) $ rectum (mucosa+wall)
C Organ: lungs
c      (35 36) $ left+right
C Organ: stomach

```

c (53 54) \$ mucosa+wall
 C Organ: urinary bladder
 c (75 76) \$ mucosa+wall
 C Organ: breast
 c (81 82) \$ left+right
 C Organ: liver
 c 44
 C Organ: esophagus
 c (49 \$ thoracic portion
 c 50 \$ abdominal portion
 c 51) \$ remainder
 C Organ: thyroid
 c 19
 C Organ: skin
 c (1 \$ head+neck
 c 84) \$ trunk
 C Organ: bone surface
 c (25 26 27 \$ C,T,L-spine
 c 28 \$ ribs
 c 29 \$ clavicles
 c 30 \$ scapulae
 c 31) \$ pelvis
 C Organ: adrenals
 c (40 41)
 C Organ: brain
 c 6
 C Organ: Extrathoracic airways
 c (9 \$ sinuses
 c 12 10 \$ pharynx (mucosa+wall)
 c 15 13) \$ larynx (mucosa+wall)
 C Organ: small intestine
 c 56
 C Organ: kidneys
 c (42 43)
 C Organ: muscle
 c 83
 C Organ: pancreas
 c 47
 C Organ: spleen
 c 48
 C Organ: thymus
 c 37
 C Organ: uterus
 c 80
 C Organ: eyes

```

c          (7 8)
C ENDORGAN
C =====
C ENDORGAN
C =====
C Detector Tally
F8:P,E 801
E8 0 1E-5 1.6E-3 10
FC8 Detector Response
c dermal dose
*F48:E (2900)
FC48 Electron and Photon dermal dose to 10 cm2 area
C =====
C ===== PROBLEM MODE & IMPORTANCES
C =====
MODE P E
IMP:P 1 173r 0
IMP:E 1 173r 0
C =====
C ===== SOURCE DESCRIPTION
C =====
SDEF POS=23.95 0 13.65 RAD=D1 PAR=E ERG=D5 CEL=608
      EFF=1E-4
SI1 0 0.2523132522 $ radial limits for source sampling
SP1 -21 2 $ uniform radial probability
si5 H
      1.0E-03 1.1E-03 1.2E-03 1.3E-03 1.4E-03 1.5E-03 1.6E-03 1.8E-03
      2.0E-03 2.2E-03 2.4E-03 2.6E-03 2.8E-03 3.0E-03 3.2E-03 3.6E-03
      4.0E-03 4.5E-03 5.0E-03 5.5E-03 6.0E-03 6.5E-03 7.0E-03 7.5E-03
      8.0E-03 8.5E-03 9.0E-03 1.0E-02 1.1E-02 1.2E-02 1.3E-02 1.4E-02
      1.5E-02 1.6E-02 1.8E-02 2.0E-02 2.2E-02 2.4E-02 2.6E-02 2.8E-02
      3.0E-02 3.2E-02 3.6E-02 4.0E-02 4.5E-02 5.0E-02 5.5E-02 6.0E-02
      6.5E-02 7.0E-02 7.5E-02 8.0E-02 8.5E-02 9.0E-02 1.0E-01 1.1E-01
      1.2E-01 1.3E-01 1.4E-01 1.5E-01 1.6E-01 1.8E-01 2.0E-01 2.2E-01
      2.4E-01 2.6E-01 2.8E-01 3.0E-01 3.2E-01 3.6E-01 4.0E-01 4.5E-01
      5.0E-01 5.5E-01 6.0E-01 6.5E-01 7.0E-01 7.5E-01 8.0E-01 8.5E-01
      9.0E-01 1.0E+00 1.1E+00 1.176E+00

sp5 D
      0.0000E+00 3.5110E-04 3.5100E-04 3.5080E-04 3.5060E-04 3.5040E-04
      3.5020E-04 7.0000E-04 6.9920E-04 6.9860E-04 6.9780E-04 6.9700E-04
      6.9640E-04 6.9560E-04 6.9480E-04 1.3880E-03 1.3852E-03 1.7275E-03
      1.7230E-03 1.7185E-03 1.7140E-03 1.7090E-03 1.7045E-03 1.7000E-03
      1.6955E-03 1.6905E-03 1.6860E-03 3.3630E-03 3.3570E-03 3.3510E-03
      3.3460E-03 3.3410E-03 3.3360E-03 3.3310E-03 6.6520E-03 6.6300E-03
      6.6100E-03 6.5900E-03 6.5700E-03 6.5480E-03 6.5280E-03 6.5080E-03

```

1.2976E-02 1.2896E-02 1.6020E-02 1.5895E-02 1.5775E-02 1.5655E-02
1.5535E-02 1.5420E-02 1.5305E-02 1.5190E-02 1.5080E-02 1.4970E-02
2.9720E-02 2.9280E-02 2.8850E-02 2.8420E-02 2.7980E-02 2.7540E-02
2.7100E-02 5.3300E-02 5.1400E-02 4.9380E-02 4.7180E-02 4.4780E-02
4.2160E-02 3.9260E-02 3.6100E-02 6.5320E-02 5.0200E-02 4.2510E-02
1.8745E-02 3.9955E-03 2.9285E-03 2.7725E-03 2.5955E-03 2.3940E-03
2.1655E-03 1.9095E-03 1.6265E-03 2.6450E-03 1.3830E-03 2.4913E-04

sb5 0.0 82i 1.0

C =====

C ===== NUMBER OF PARTICLES

C =====

print 110

NPS 5.0E6

c PRDMP 1.0E3 100 0 1

REFERENCES

- [1] Radiation Studies Branch, Division of Environmental Hazards and Health Effects, National Center for Environmental Health, Centers for Disease Control and Prevention, U.S. Department of Health and Human Services, "Population monitoring in radiation emergencies: A guide for state and local public health planners," Apr. 2014.
- [2] Federal Emergency Management Agency, "FEMA-REP-21: Contamination Monitoring Standard for a Portal Monitor Used for Radiological Emergency Response," Mar. 1995.
- [3] R. Ricks, M. Berger, E. Holloway, and R. Goans, "Reac/ts radiation accident registry: Update of accidents in the united states," *IRPA-10 Proceedings of the 10th international congress of the International Radiation Protection Association on harmonization of radiation, human life and the ecosystem*, 2000.
- [4] G. Bugliarello, "Nuclear dangers," *The Bridge*, vol. 40, pp. 3–4, 2 2010.
- [5] T. Tenforde, D. Schauer, R. Goans, F. Mettler Jr., T. Pellmar, J. Poston Sr., and T. T., "Health aspects of a nuclear or radiological attack," *The Bridge*, vol. 40, pp. 50–57, 2 2010.
- [6] L. Shankar, "Radiological and nuclear emergencies: Medical management of radiation injuries," *Defence Science Journal*, vol. 61, pp. 113–117, 2 Mar. 2011.
- [7] National Security Staff Interagency Policy Coordination Subcommittee for Preparedness & Response to Radiological and Nuclear Threats, "Planning guidance for response to a nuclear detonation," Jun. 2010.
- [8] H. Kondo, J. Shimada, C. Tase, T. Tominaga, H. Tatsuzaki, M. Akashi, K. Tanigawa, Y. Iwasaki, T. Ono, M. Ichihara, Y. Kohayagawa, and Y. Koido, "Screening of residents following the tokyo electric fukushima daichi nuclear power plant accident," *Health Physics*, vol. 105, pp. 11–20, 1 Jul. 2013.
- [9] Radiation Emergency Assistance Center/Training Site [REAC/TS], "The medical aspects of radiation incidents," Jul. 2017.
- [10] The International Atomic Energy Agency and The World Health Organization, "Safety reports series no. 2: Diagnosis and treatment of radiation injuries," May 1998.

- [11] R. Shore, “Overview of radiation-induced skin cancer in humans,” *Int. J. Radiat. Biol.*, vol. 57, pp. 809–827, 4 Apr. 1990.
- [12] G. Thibodeau and K. Patton, *Anatomy & Physiology*, 6th ed. Mosby Elsevier, 2007.
- [13] H. Cember and T. Johnson, *Introduction to Health Physics*, 4th ed. The McGraw-Hill Companies, 2009.
- [14] J. Whitton, “New values for epidermal thickness and their importance,” *Health Physics*, vol. 24, pp. 1–8, Jan. 1973.
- [15] J. Whitton and J. Everall, “The thickness of the epidermis,” *British Journal of Dermatology*, vol. 89, pp. 467–476, Apr. 1973.
- [16] J. Sandby-Moller, T. Poulsen, and H. Christian Wulf, “Epidermal thickness at different body sites: Relationship to age, gender, pigmentation, blood content, skin type and smoking habits,” *Acta Derm Venereol*, vol. 83, pp. 410–413, Jun. 2003.
- [17] The International Commission on Radiological Protection, “Icrp publication 89: Basic anatomical and physiological data for use in radiological protection: Reference values,” *Annals of the ICRP*, vol. 32, 3-4 2002.
- [18] M. Thoolen, T. Ryan, and I. Bristow, “A study of the skin of the sole of the foot using high-frequency ultrasonography and histology,” *The Foot*, vol. 10, pp. 14–17, 2000.
- [19] National Cancer Institute. (). Seer training modules: Layers of the skin [online], (visited on 03/27/2018).
- [20] M. Charles, “Radon exposure of the skin: I. biological effects,” *Journal of Radiological Protection*, vol. 27, pp. 231–252, 3 2007.
- [21] P. Covens, D. Berus, V. Caveliers, L. Struelens, F. Vanhavere, and D. Verellen, “Skin dose rate conversion factors after contamination with radiopharmaceuticals: Influence of contamination area, epidermal thickness and percutaneous absorption,” *Journal of Radiological Protection*, vol. 33, pp. 381–393, 2013.
- [22] F. Attix, *Introduction to Radiological Physics and Radiation Dosimetry*. John Wiley & Sons, Inc., 1986.
- [23] M. Stabin, *Radiation Protection and Dosimetry*. Springer Science+Business Media, LLC, 2007.
- [24] S. Sugarman, “Early internal and external dose magnitude estimation,” 2017.

- [25] A. Ansari, *Radiation Threats and Your Safety: A Guide to Preparation and Response for Professionals and Community*, ? Taylor and Francis Group, LLC, 2010.
- [26] National Institute of Standards and Technology. (). ESTAR: Stopping Power and Range Tables for Electrons [online], (visited on 03/27/2018).
- [27] C. Riland, “Emergency response instrumentation,” *Radiation Instruments*, pp. 289–301, 2001.
- [28] G. Knoll, *Radiation Detection and Measurement*, 4th ed. John Wiley & Sons, Inc., 2010.
- [29] N. Tsoulfanidis and S. Landsberger, *Measurement and Detection of Radiation*, 3rd ed. Taylor and Francis Group, LLC, 2011.
- [30] P. Steinmeyer, “G-m panckae detectors: Everything you’ve wanted to know (but were afraid to ask),” *RSO Magazine*, vol. 10, pp. 7–17, 5 2005.
- [31] Federal Emergency Management Agency, “Background Information on FEMA-REP-21: Contamination Monitoring Standard for a Portal Monitor Used for Radiological Emergency Response,” 1995.
- [32] S. Hoath and D. Leahy, “The organization of human epidermis: Functional epidermal units and phi proportionality,” *The Journal of Investigative Dermatology*, vol. 121, pp. 1440–1446, 6 Dec. 2003.
- [33] Federal Emergency Management Agency, “Improvised nuclear device response and recovery: Communicating in the immediate aftermath,” Jun. 2013.
- [34] D. Peel, J. Hopewell, J. Wells, and M. Charles, “Nonstochastic effects of different energy beta emitters on pig skin,” *Radiation Research*, vol. 99, pp. 372–382, 2 Aug. 1984.
- [35] J. Coggle, L. Hansen, J. Wells, and M. Charles, “Nonstochastic effects of different energy beta emitters on mouse skin,” *Radiation Research*, vol. 99, pp. 336–345, 2 Aug. 1984.
- [36] J. Fowler, “Volume effects in radiobiology as applied to radiotherapy,” *J. Jpn. Soc. Ther. Radiol. Oncol.*, vol. 5, pp. 75–87, 1993.
- [37] F. Devik, “Cell migration following irradiation of the skin in mice: Effect of shielding minute areas,” *Acta Radiologica: Therapy, Physics, Biology*, vol. 16, pp. 257–265, 3 1977.

- [38] Federal Emergency Management Agency, “FEMA-REP-21: Contamination Monitoring Standard For A Portal Monitor Used For Radiological Emergency Response,” Mar. 1995.
- [39] Federal Emergency Management Agency, “FEMA-REP-22: Contamination Monitoring Guidance For Portable Instruments Used For Radiological Emergency Response To Nuclear Power Plant Accidents,” Oct. 2002.
- [40] Federal Emergency Management Agency, “Background Information on FEMA-REP-22: Contamination Monitoring Guidance For Portable Instruments Used For Radiological Emergency Response To Nuclear Power Plant Accidents,” Oct. 2002.
- [41] Conference of Radiation Control Program Directors, Inc., “Handbook for Responding to a Radiological Dispersal Device: First Responder’s Guide–The First 12 Hours,” Sep. 2006.
- [42] Office of Radiation and Indoor Air, Radiation Protection Division, U.S. Environmental Protection Agency, “EPA-400/R-17/001: PAG Manual: Protective Action Guides and Planning Guidance for Radiological Incidents,” Jan. 2017.
- [43] Office of Radiation Programs, United States Environmental Protection Agency, “Manual of Protective Action Guides and Protective Actions for Nuclear Incidents,” May 1992.
- [44] International Atomic Energy Agency, “Operational Intervention Levels for Reactor Emergencies and Methodology for Their Derivation,” Mar. 2017.
- [45] National Council on Radiation Protection and Measurement (NCRP), “Management of Persons Contaminated with Radionuclides: Handbook (Report No. 161),” Dec. 2008.
- [46] National Council on Radiation Protection and Measurement (NCRP), “Responding to a Radiological or Nuclear Terrorism Incident - A Guide for Decision Makers (Report No. 165),” Jan. 2010.
- [47] National Council on Radiation Protection and Measurement (NCRP), “Population Monitoring and Radionuclide Decorporation Following a Radiological or Nuclear Incident (Report No. 166),” Apr. 2010.
- [48] H. Akkurt and K. Eckerman, “Development of PIMAL: Mathematical Phantom with Moving Arms and Legs,” May 2007.
- [49] R. Manger, “Assessing the Dose Received by the Victims of a Radiological Dispersal Device with Geiger-Mueller Detectors,” Aug. 2008.

- [50] W. Bloch, J. Hurtado, C. Lee, R. Manger, E. Burgett, N. Hertel, and W. Dickerson, “Guidance on the Use of Handheld Survey Meters for Radiological Triage: Time-Dependent Detector Count Rates Corresponding to 50, 250, and 500 mSv Effective Dose for Adult Males and Adult Females,” *Health Physics*, vol. 102, pp. 305–325, 3 2012.
- [51] International Atomic Energy Agency, “The Radiological Accident in Goiânia,” Sep. 1988.